MICROWAVE AND CONVENTIONAL SINTERING OF MANGANESE-DOPED ALUMINA: DENSIFICATION AND MECHANICAL PROPERTIES

SALEM BIN DHUBAN

FACULTY OF ENGINEERING
UNIVERSITY OF MALAYA
KUALA LUMPUR

2019

MICROWAVE AND CONVENTIONAL SINTERING OF MANGANESE-DOPED ALUMINA: DENSIFICATION AND MECHANICAL PROPERTIES

SALEM BIN DHUBAN

DISSERTATION SUBMITTED IN FULFILMENT OF
THE REQUIREMENTS FOR THE DEGREE OF MASTER
OF ENGINEERING SCIENCE

FACULTY OF ENGINEERING
UNIVERSITY OF MALAYA
KUALA LUMPUR

2019

UNIVERSITY OF MALAYA
ORIGINAL LITERARY WORK DECLARATION

Name of Candidate: Salem Omar Abdullah Bin Dhuban

Matric No: KGA170010

Name of Degree: Master of Engineering Science

Title of Project Paper/Research Report/Dissertation/Thesis ("this Work"):

Microwave and Conventional Sintering of Manganese-Doped Alumina: Densification And Mechanical Properties

Field of Study:

I do solemnly and sincerely declare that:

(1) I am the sole author/writer of this Work;
(2) This Work is original;
(3) Any use of any work in which copyright exists was done by way of fair dealing and for permitted purposes and any excerpt or extract from, or reference to or reproduction of any copyright work has been disclosed expressly and sufficiently and the title of the Work and its authorship have been acknowledged in this Work;
(4) I do not have any actual knowledge nor do I ought reasonably to know that the making of this work constitutes an infringement of any copyright work;
(5) I hereby assign all and every rights in the copyright to this Work to the University of Malaya ("UM"), who henceforth shall be owner of the copyright in this Work and that any reproduction or use in any form or by any means whatsoever is prohibited without the written consent of UM having been first had and obtained;
(6) I am fully aware that if in the course of making this Work I have infringed any copyright whether intentionally or otherwise, I may be subject to legal action or any other action as may be determined by UM.

Candidate's Signature Date:

Subscribed and solemnly declared before,

Witness's Signature Date:

Name:

Designation:

MICROWAVE AND CONVENTIONAL SINTERING OF MANGANESE-DOPED ALUMINA: DENSIFICATION AND MECHANICAL PROPERTIES

ABSTRACT

The effect of manganese as a densification enhancing additive in alumina was studied. Various manganese percentages (0.1, 0.5, and 1.0 wt. %) were added to alumina powder. The mixture was homogenized using wet milling process. Sintering was carried out in conventional furnace and in hybrid multimode microwave furnace. XRD analysis revealed the precipitation of a spinel second phase ($MnAl_2O_4$) in manganese-doped samples as a result of manganese limited solubility in the corundum lattice. 0.1 wt. % manganese addition significantly enhanced the densification process, hindered grain growth, and improved hardness of alumina sintered at 1500 °C. At 1500 °C, 97.5 % relative density was obtained for alumina with 0.1 wt. % manganese content, whereas undoped alumina could only achieve 94.2 % relative density. 0.5 and 1.0 wt. % manganese concentrations resulted in abnormal grain growth at high sintering temperature (1600 °C). The study also revealed that microwave sintering was effective in suppressing grain growth of alumina. In addition, the hardness was dependent on the sintered bulk density and that grain coarsening ensued as the density of the sintered alumina exceeded 95% of theoretical.

Keywords**:** Alumina; Sintering additive; Manganese doping; Microwave sintering; Conventional sintering

PERSINTERAN KONVENSIONAL DAN GELOMBANG MIKRO ALUMINA TERDOP MANGAN: PENUMPATAN DAN SIFAT MEKANIKAL

ABSTRAK

Kesan penambahan mangan ke dalam alumina sebagai bahan penggalak pemadatan telah dikaji. Bagi tujuan ini, pelbagai peratusan mangan (0.1, 0.5, dan 1.0 wt.%) telah ditambah kepada serbuk alumina. Campuran itu dihomogenisasi menggunakan proses penggilingan basah. Proses persinteran dijalankan dalam relau konvensional dan dalam relau hibrid bergelombang mikro multimod. Analisis XRD mendedahkan pemendakan fasa kedua spinel ($MnAl_2O_4$) telah terhasil di dalam sampel-sampel alumina yang didopakan, akibat kelarutan terhad mangan dalam kekisi korundum. Tambahan sebanyak 0.1 wt.% mangan menunjukkan peningkatan ketara bagi proses persinteran, menghalang pertumbuhan butiran, dan meningkatkan kekerasan alumina pada suhu 1500 °C. Pada suhu ini, ketumpatan relatif setinggi 97.5% diperolehi untuk alumina dengan kandungan mangan 0.1 wt. %, manakala alumina yang tidak didopakan hanya dapat mencapai kepadatan relatif 94.2%. Kandungan mangan sebanyak 0.5 dan 1.0 wt. % mengakibatkan pertumbuhan butiran yang tidak normal pada suhu persinteran yang tinggi (1600 °C). Kajian ini juga mendedahkan bahawa proses persinteran bergelombang mikro berkesan dalam menahan pertumbuhan butiran alumina. Di samping itu, kekerasan alumina yang dipadatkan melalui proses persinteran bergantung pada ketumpatan pukal dan kekasaran butiran pula berlaku kerana ketumpatan alumina melebihi 95% daripada nilai teori.

Keywords: Alumina: Bahan tambahan sintering; Mangan terdop; Persinteran konvensional; Gelombang mikro

ACKNOWLEDGEMENTS

First and foremost, I would like to thank my supervisor Professor Ir Dr. Ramesh Singh for providing me with the opportunity to work on this exciting project and for his kind and patient support throughout the duration of this study.

Secondly, I would like to thank Hadhramout Foundation, and very special thanks to Eng. Abdullah Ahmed Bugshan, founder and head of Hadhramout Foundation, for their financial support which without I probably would not be able to further my study to this level.

Several former and current members of the Professor Ramesh's lab have contributed invaluably to the presented work through numerous scientific discussions as well as technical assistance, but most importantly through their warm friendship and kind hearts. Sara Lee, Malihah Amiri Roudan, Auwal Shamsu Tukur, Tawfik Al-Habla, and Husna Zulkifli, it has been a true privilege and a great pleasure working with you and calling you my friends.

Additionally, I would like to thank SIRIM Berhad for their help in the experiments.

My family in Yemen, I thank you from the bottom of my heart. Without your continuous encouragement and your patience throughout the years I wouldn't be writing this thesis.

TABLE OF CONTENTS

LIST OF FIGURES

LIST OF TABLES

LIST OF SYMBOLS AND ABBREVIATIONS

Al_2O3 : Aluminum oxide or alumina

SPS : Spark plasma sintering

TiO_2 : Titanium oxide or titania

ZrO_2 : Zirconium oxide or zirconia

Y_2O_3 : Yttrium oxide or yttria

MgO : Magnesium oxide or magnesia

CeO_2 : Cerium oxide or ceria

γ : Interface energy

R : Gas constant

T : Temperature

$\mathit{\Gamma}$: Gibbs excess energy

AGG : Abnormal grain growth

CaO : Calcium oxide

SiO_2 : Silicon oxide or silica

SrO : Strontium oxide or strontia

BaO : Barium oxide

NaO : Sodium Oxide

Wt. % : Weight Percent

Al_2TiO_5 : Aluminum titanate

XRD : X-Ray diffraction

SEM : Scanning electron microscope

YSZ : Yttria-stabilized zirconia

HA : Hydroxyapptite

TCP	:	Tricalcium phosphate
SiC	:	Silicon carbide
3-YSZ	:	3 mol % yttria-stabilised zirconia
ZnO	:	Zinc oxide
$Al_5Y_3O_{12}$	:	Yttrium aluminum garnet
MnO_2	:	Manganese dioxide
ρ	:	Density
CIP	:	Cold isostatic pressing
JCPDS	:	Joint Committee of Powder Diffraction Standard
ICCD	:	International Centre for Diffraction Data
$MgAl_2O_4$	:	Magnesium aluminate
EDS		Energy-dispersive X-ray spectroscopy

CHAPTER 1: INTRODUCTION

Aluminium oxide (Al_2O_3), known as alumina is the most widely used engineering ceramic material. In its single crystal form, alumina is used in watch bearings and pressure resistant window. Alumina processed by hot-pressing methods is employed as electrical insulators, windows or radomes transparent to microwaves, envelopes for lamps and electrical devices. Polycrystalline alumina is the basis for refractory bricks, crucibles and spark plug insulators (Carter & Norton, 2007).

Generally, ceramic materials are difficult to fabricate. Ceramics are fabricated using powder metallurgy processing techniques in which the starting material is in a form of powder, and compaction techniques are necessary to shape the desired body. After compaction, the obtained "green body" usually has relative density of ≈ 50% (the relative density is a percentage of the actual density of the body relative to the theoretical density of fully-dense body). The green body must then be sintered at relatively high temperatures and for relatively long times in order to achieve full consolidations. According to Castro and van Benthem (2012) "sintering is exploited to consolidate particles with controlled porosity by heating a compact at around 2/3 of its melting point". Heating a material to this temperature allows the necessary significant atomic mobility to establish sintering conditions.

Traditionally, ceramics are sintered in electric furnaces at temperatures well above 1000 °C with hours of isothermal dwell time at the sintering temperature to allow the atomic diffusion to occur, and thus the densification process. In particular, dense alumina ceramics are typically obtained at temperatures exceeding 1500 °C and this temperature can be even higher (up to 1800 °C), if coarse starting powder is used (Li et al., 2017).

High sintering temperatures and long holding times increase energy consumption during the heating process, increase the production cycle time, and induce undesired grain growth (Krell & Blank, 1996).

During heating of ceramics, when the diffusion of atoms is high enough, three simultaneous processes start to happen which are: sintering, coalescence and grain growth (Castro & van Benthem, 2012). Sintered bodies usually contain residual pores which result from discontinuous grain growth, that is, the rapid growth of some grains causes pores to be trapped within them. Polycrystalline ceramics consist of multiple grains, grain size and orientation play a major role in determining the properties of these materials at the macroscopic level. Controlling grain growth provides a way to control a material's properties. Microstructure of ceramics is influenced by the way it was processed. For instance, ceramics sintered using pressure assisted techniques (Muche et al., 2017) contain less pores than pressureless sintered ceramics, and ceramics containing minute percentages of metal oxide additives (Dillon & Harmer, 2008) might show a densification process or possess grain size different from that of pure ceramics.

Therefore, extensive research has been done over the last decades to develop processing techniques for the preparation of fully-dense ceramic materials with controlled microstructure, enhanced mechanical and physical properties, reduced sintering temperatures, and shortened sintering time. These techniques include field activated sintering technique (FAST) (e. g. spark plasma sintering, SPS) (Munir et al., 2006), microwave sintering (Demirskyi et al., 2013), two-step sintering (Lóh et al., 2016; Chang & Wang, 2000), and the use of sintering additives (e. g. magnesium oxide) (Ehre & Chaim, 2008).

Field activated sintering process, such as spark plasma sintering (SPS) are powerful techniques for obtaining dense fine-grained ceramics at low temperatures. In Field activated sintering, compacts are consolidated by the aid of applied pressure and joule heating. Joule heating is beneficial in by-passing low temperature grain growth, whereas pressure facilitates particle rearrangement (Munir et al., 2006). SPS was used to obtain highly dense transparent alumina at only 800 °C, but using 7.7 GPa of pressure (Nishiyama et al., 2013). Pressure-assisted techniques, however, are costly to setup and the shape of the produced material is restricted to the shape and size of the die which preventing its use for mass production. Hence, a more affordable and more flexible sintering technique is needed for mass production.

One of newly emerging techniques is microwave processing of ceramic materials. Microwave sintering was the subject of many studies over the last three decades and it has shown many advantages over conventional furnaces. The main advantage of microwave sintering is its ability to heat the material volumetrically, whereas in conventional furnace, heat is transferred into the material by means of conduction, convection and radiation. Volumetric heating in microwave sintering enabled high heating rates to be applied, energy saving, and reduced sintering time. Other reported advantages of microwave sintering over conventional sintering are: reduction of the effective sintering temperatures, enhanced atom diffusion, and enhanced mechanical and physical properties (Oghbaei & Mirzaee, 2010).

Transitional metal oxides, such as MgO and TiO_2, are commonly used as sintering additives in many ceramic materials. Small amounts (ppm) of these dopants are added to the solute material in order to affect the resultant material’s macroscopic properties. It is believed that sintering additives aid the densification process through: (1) reducing the sintering temperature and time needed for the completion of densification, (2) promoting densification by inhibiting discontinuous grain growth.

Dopants were shown to enhance densification rate and lower the effective sintering temperature (Erkalfa et al., 1995; Xu et al., 2017), suppress grain growth (Pereira et al., 2017), improve the mechanical and physical properties of many ceramic materials. MgO is the most widely studied sintering additive for alumina (Maca et al., 2014). MgO, however, does not lower the sintering temperature of alumina, instead it supresses grain growth of alumina (Bodišová et al., 2015). Y_2O_3 and ZrO_2 are also commonly studied dopants for alumina, but according to Maca et al. (2014), both dopants significantly inhibit densification of alumina. Another dopant is manganese which was recently reported to significantly enhanced the densification of yttria-stabilized zirconia (Li et al., 2017), yttria-tetragonal zirconia polycrystals (Ramesh et al., 2008), and ceria (Wu et al., 2015; Wu et al., 2014; Zhang et al., 2003). Although, manganese was deemed an effective sintering additive for number of ceramic materials, studies on manganese-doped alumina are rather limited. The last study was published in the year of 2002 by Sathiyakumar and Gnanam. Conventional sintering was used in this study, and insignificant difference in relative densities between manganese-doped and pure alumina samples was reported (Sathiyakumar & Gnanam, 2002).

Due to the reported effectiveness of manganese as densification enhancing additive. The aim of this study is to investigate the effect manganese on the densification, and mechanical properties of alumina. In addition to conventional sintering, samples will be sintered in microwave furnace for comparison.

1.1 Problem Statement

Alumina ceramics attain their excellent properties at extremely high temperatures and long holding times. High temperatures and long holding time increase grain growth and devour energy. Grain growth negatively affect the mechanical properties of ceramic materials. Most of the published studies focused on influencing the densification mechanisms through the addition of specific sintering additives including MgO, TiO_2, Y_2O_3, and ZrO_2. Effects of MgO on the densification and mechanical properties of alumina was the subject of a vast number of published research. Furthermore, the literature contains a good number of published research that focused on the effects of TiO_2, Y_2O_3, or ZrO_2 on the densification and mechanical properties of alumina. Manganese, on the other hand, is an overlooked dopant for alumina as it has been shown to enhance the densification process and improve the mechanical properties of other ceramic materials, such as zirconia and ceria, but the number of studies on manganese-doped alumina are scarce and lacking.

1.2 Objectives

The objectives of this study were:

1. To investigate the effect of manganese oxide (MnO_2) addition on the densification, microstructural evolution, and hardness of alumina.
2. To investigate the effect of microwave sintering on the densification, microstructural evolution, and hardness of alumina.

1.3 Scope of the Study

This study focuses on two main aspects: (1) densification and mechanical properties of manganese-doped alumina, and (2) effect of microwave sintering on the densification and mechanical properties of manganese-doped alumina. Manganese-doped and undoped samples will be prepared using an established wet milling method. Undoped and manganese-doped samples will be sintered using both microwave furnace and conventional furnace. Conventional sintering will be carried out at 1300, 1400, and 1500, and 1600 °C. Microwave sintering will be carried out at 1300, 1400, and 1500 °C. Constant heating rates and cooling rates will be applied: 10 °C /min for conventional sintering, and a heating rate of 30 °C/min for microwave sintering. Isothermal dwell time of 2 hours will be applied for conventional sintering, and a 5-min isothermal dwell time for microwave sintering. Vickers hardness will be determined and related to the density, phases and microstructure of the sintered bodies.

1.4 Thesis Structure

This thesis is divided into five chapters: introduction, literature review, methodology, results and discussion, and conclusions and future work.

Chapter one is the Introduction chapter. It contains broad background about ceramics and alumina ceramic in particular, how the ceramics are processed and basic definitions that are necessary for the reader to understand the topic are also presented in the introductory chapter. This chapter paves the way for the reader to understand the topic of the thesis and its importance. The chapter concludes with the problem statement, objective and scope of the study.

Chapter two is on the literature review of this research. This chapter is divided into two main sections: sintering additives and microwave sintering. The sintering additives section introduces the use of sintering additives and their basic working mechanisms. The literature review covers the most commonly used sintering additives for alumina, i. e. MgO, Y_2O_3, and TiO_2. In addition, the use of manganese as an additive for other ceramic materials is presented. The second section, microwave sintering details the use of microwave sintering for ceramics.

Chapter three is the research methodology, which details the procedures adopted in this study. The experimental procedure includes green sample preparation, sintering, density evaluation, grinding and polishing, X-Ray diffraction analysis, Vickers Hardenss test and microstructural evaluation.

Chapter four is the results and discussions, which presents the findings of this study and relate it to the available relevant literature. This chapter is divided into two main sections. The first section is on the manganese effect on the densification and hardness of alumina. The second section is microwave sintering and conventional sintering comparison, which contrasts the results that were obtained using both methods.

Chapter five presents the conclusions and further work.

CHAPTER 2: LITERATURE REVIEW

Economically sintered ceramics with unique combination of high hardness, high density, and thermodynamic stability has been the subject of many studies (Wollmershauser et al., 2014). Alumina is one of the widely used ceramic materials because of its temperature resistance, wear and deformation resistance. It is used for various engineering and biomedical applications, such as thread guides, cutting tools and hip implants (Carter & Norton, 2007). Therefore, extensive researches has been made over the last decades to develop processing techniques for the preparation of dense alumina ceramics with engineered microstructure.

Dense fine-grained ceramics exhibit unusual properties due to the abnormally large number of atoms associated with the grain boundaries. Ceramics follow the Hall–Petch relationship from which a material strength and hardness increase with decreasing grain size (Hall, 1951; Wollmershauser et al., 2014). Unlike metals, ceramics deos not show a decrease in hardness below certain grain size limit (Muche et al., 2017). Due to the unusual properties of fine-grained ceramics, many of the recently published studies focused on the development of processing techniques to enhance densification while controlling grain growth. Fine-grained ceramics are mostly processed using pressure assisted techniques, such as spark Plasma Sintering which was used to prepare fine-grained zirconia (Dey et al., 2016) and $MgAl_2O_4$ spinel (Muche et al., 2017; Wollmershauser et al., 2014). Hot Isostatic Press (HIP) was used for the production of nanostructured transparent alumina under 7.7 GPa of pressure and sintering temperature of 800 °C (Nishiyama et al., 2013). Although Pressure-assisted sintering methods are capable of producing highly dense fine-grained ceramics at low temperatures, the complexity and cost of the equipment used are preventing these techniques from being adopted for mass production. Adding impurities into the solvent material is an established way for improving the densification process, and microstructure engineering.

2.1 Sintering Additives

The addition of transitional metal oxides in minute amounts is an effective way to influence the microstructural evolution and the resulting properties of polycrystalline materials (Galusek et al., 2012). Improved densification rates, lower effective sintering temperatures (Lahiri et al., 2016), and grain growth supression (Bodišová et al., 2015; Dey et al., 2016) were accomplished using sintering additives.

Dopants added to a solvent material may segregate to the grain boundaries, segregate to the surface, form a second phase, or form a solid solution with the host material (Li et al., 2017; Rahaman & Zhou, 1995). Dopants that segregate to the grain boundaries are expected to effect the kinetics of grain boundaries movement and increase its activation energy through grain boundary pinning effect or solute drag. This phenomenon is attributed to the difficulty in moving boundaries containing dopants and the cloud of defects surrounding it caused by charge compensation and lattice mismatch between dopant and matrix (Kirchheim, 2002; Wu et al., 2015). For instance, the effect of multiple dopants (Mg^{2+}, Ca^{2+}, and Y^{3+}) on the grain boundary mobility of CeO_2 was studied by Chen and Chen (1996). They found that segregation of dopants cations slowed down grain boundary mobility at high dopant concentrations due solute drag effect. Some other dopants show a change in their valence state upon heating, such as manganese, which was shown to increase grain boundary mobility (Li et al., 2017).

From thermodynamic point of view, dopants enriched grain boundaries inhibit grain growth through the reduction of Gibbs free energy of the host material which is the driving force for coarsening (Kirchheim, 2002; Weissmüller, 1993) according to the following equation (1):

$$d\gamma = RT\Gamma_{2,1} d\ In\ X_2 \qquad (1)$$

Subscripts “1” and “2” represent solvent (host material) and solute (dopant), respectively, γ is the interface energy, R is the gas constant, T is temperature, Γ is Gibbs excess of the interface and X_2 is the molar fraction of the solute in the bulk (Wu et al., 2015). Therefore, increasing the solute segregation to a certain limit can bring the grain boundary energy to an equilibrium state and enabling the control of grain growth (Castro et al., 2015). Professor Castro and his research group succeed in measuring and reducing the grain boundary energy of gadolinium-doped nanocrystalline zirconia to quasi-zero state. They used an ultrasensitive microcalorimetry to prove the theoretical calculations that grain boundary energy can become zero as a function of dopant concentration (Nafsin & Castro, 2016). In another work, they found out that grain size of ceria decreased with increasing Mn^{3+} dopant content due to the decrease in the free energy caused by dopant segregation (Wu et al., 2014). Thus, dopants can affect the kinetics and thermodynamics associated with coarsening providing a way to control grain growth during sintering. Surprisingly, sintering additives are selected based on trial and error approach as there is no scientific bases to support the selection (Dillon et al., 2010). In this review, some of the commonly studied sintering additives for alumina, such as MgO, Y_2O_3, TiO_2, ZrO_2, will be reviewed. Also studies concerning manganese effects on the sintering behavior of various ceramic materials will be reviewed.

2.1.1 Magnesium Oxide

Magnesium oxide or magnesia (MgO) is undoubtedly the most studied dopant. Ever since it was first reported by Coble (1962) that small amount (0.25%) of MgO enhanced the densification of alumina to near theoretical density, there has been substantial number of studies on the quest to understand the mechanisms underlying it and to further explore its effect on the densification of alumina. It is believed that MgO supresses pore-boundary separation, reduces grain growth, and eliminates anisotropic grain growth in alumina. Yet, still there is a controversy about the mechanisms which enable such high densities to be attained, and whether MgO is a densification enhancer or inhibitor, grain growth promoter or suppressor.

The early studies focused on the role of MgO in limiting inhomogeneous grain boundary segregation of impurities and the subsequent anisotropic grain growth. In alumina it is generally believed that abnormal grain growth (AGG) is caused by the presence of liquid-phase-forming impurities in alumina powder, such as sodium oxide (Patrick & Cutler, 1965), SiO_2, CaO_2, and TiO_2 (Hyeon & Yeon, 2001). These impurities segregate to the grain boundaries and their accumulation increase with grain size, until grain size reaches a critical value, impurity concentration exceeds the solubility limit in alumina and intergranular liquid film appears. This liquid film was suggested to trigger AGG by increasing grain boundary mobility (Bae & Baik, 1997; Bae & Baik, 1993). Inhomogeneous grain growth can result in various grain sizes and shapes (Huesup & Coble, 1990):

(1) platelike grains are a type of abnormal grain, usually ≥ 100 μm in length, with aspect ratio ≥ 5 and the boundaries parallel to the long axis are straight.

(2) Platelet grains: these grains have straight boundaries but the size of the grains on order of 10 μm or less.

(3) Elongated grains: grains with aspect ratio > 2.

(4) Equiaxed grains: grains with aspect ratio < 2.

MgO doping affects the AGG phenomenon in alumina. According Baik and Moon (1991), MgO enhanced the chemical homogeneity of commercial alumina. Inhomogeneous segregation of Ca (Ca is commonly present in commercial alumina as impurity material) to the grain boundaries of alumina was detected, but doping alumina with MgO resulted in a more homogeneous segregation of Ca to the grain boundaries and more homogeneous grain growth. In another related study, Handwerker et al. (1989) found that the presence of MgO as a solute in alumina reduced the effect of chemical inhomogeneity – that is, the inhomogeneous segregation of impurities to the grain boundaries – and mitigated discontinuous grain growth which was observed in undoped alumina. The reduction in the chemical inhomogeneity was attributed to the increase in the bulk solubility and the subsequent decrease in the interfacial segregation caused by the MgO addition.

Gavrilov et al. (1999) described MgO as a liquid phase “scavenger”. They observed that segregation of Si to the grain boundaries of alumina was greatly reduced by MgO addition causing Si to form a solid solution with alumina instead of segregation to the grain boundaries. This beneficial effect was attributed to enhanced solubility of liquid-phase-forming impurities in alumina caused by the addition of MgO, thus reducing the interfacial segregation and causing liquid-phase-forming impurities to form a solid solution in MgO-doped alumina (Gavrilov et al., 1999; Handwerker et al., 1989; Zhao & Harmer, 1987).

Huesup and Coble. (1990) studied the origins and growth kinetics of abnormal grain growth behaviour in alumina with special attention to plate-like grains. Single doping and co-doping was used to examine the effect of various doping oxides on the abnormal grain growth kinetics. They observed that plate-like grains developed only in some co-doped compacts. These co-dopants include: CaO+SiO_2, SrO + SiO_2, BaO + SiO_2 or NaO + SiO_2 with doping content of 0.25 mol%. Furthermore, codoping with MgO resulted in equiaxed grains that grow at much slower rate than that of platelike grains. It was concluded that MgO reduces the anisotropy of alumina microstructure. Kim et al. (2007) achieved better microstructural homogenization and better translucency by doping alumina with MgO. The improved transmittance was attributed to the removal of residual pores at the later stages of sintering caused by the addition of MgO.

Bennison and Harmer (1983) studied the grain growth of fully dense single crystalline alumina and fully dense single crystalline MgO-doped alumina. The objective was to clarify the role of MgO on the grain growth of alumina. They found that MgO retarded the rate of grain boundary migration by a factor of five. Bernardgranger and Guizard (2007) reported finer microstructure for a given density (that is, the grain size/density trajectory) in MgO-doped alumina relative to undoped alumina. Bodišová et al. (2015) found that the combination of MgO doping and two-step sintering which was originally developed by Chang and Wang (2000) resulted in a complete suppression of grain growth during the final sintering stage of alumina at densities exceeding 99% where grain growth is most severe. The complete suppression of grain growth was attributed to the MgO segregation to the grain boundaries of alumina. Galusek et al. (2012) observed the same positive effect of MgO on grain growth reduction during the final stage of sintering.

On the other hand, some other studies reported an accelerated grain growth in MgO-doped alumin. Berry and Harmer (1986) found that MgO accelerated the grain growth rate by a factor of 2.5, whereas other studies found that the sintering path (grain size versus density trajectory) was not affected by the presence of MgO in alumina (Berry & Harmer, 1986; Radonjić & Srdić, 1997).

The MgO effect on the grain growth process is concentration-dependant. The amount of MgO solute in alumina determines whether MgO acts as grain growth supressing or grain growth enhancing agent. When MgO is added to alumina in small concentrations, it can promote grain growth. Scott et al. (2002) prepared a single crystalline alumina from polycrystalline alumina by doping alumina with small concentration (50 ppm) of MgO. At this very low concentration, AGG was promoted at the early stage of sintering. Chan et al. (1998) studied the effects of MgO doping in controlling grain growth of alumina in the presence of adequate amounts of liquid-phase-forming impurities (CaO and SiO_2). This study found that at high quantities of liquid-phase at which all grain boundaries and junctions were penetrated, MgO was not beneficial in controlling the evolution of alumina microstructure into elongated grains, whereas high concentrations of MgO causing precipitation of $MgAl_2O_4$ hindered the development of elongated grains. This beneficial effect of MgO was explained by solute drag pinning of the fast moving boundaries. More recently, Kim et al. (2003) found that MgO acts as a grain growth promoter when added in low concentrations (<200 ppm). At low concentrations (50 ppm and 100 ppm) alumina grains grew enormously, but when the concentration of MgO increased to 200 ppm, the overall grain growth was accelerated and the microstructure was homogenous without AGG. The concentration at which MgO supressed AGG corresponding to the solubility limit of MgO in alumina as demonstrated by Greskovich and Brewer (2001). In this study alumina was doped with MgO (0 – 350 ppm) using liquid immersion method. Samples were fired at temperatures ranging from 1700 – 2000 °C. The solubility of MgO in alumina was found to be temperature-dependent and was 175 ppm at 1880 °C.

On the densification rate of MgO-doped alumina, Ikegami et al. (2010), found that the densification is proportional to the surface tension and doping alumina with MgO reduced the surface tension and the shrinkage rate, and therefore reduced the densification rate of alumina. Maca et al. (2010) reported that the grain refinement in MgO-doped alumina comes at the expense of decelerated densification. Maca et al. (2014) found that MgO-doped alumina showed higher activation energy of densification in comparison to undoped alumina.

On the other hand, other studies claimed that MgO is a densification-enhancing additive. Berry and Harmer (1986) claimed that when MgO was added as a sintering additive in alumina, both the densification rate and grain growth rate were enhanced by the presence of MgO. Other study found that the presence of MgO accelerated the densification rate of alumina by a factor of 3. This effect was attributed to the accelerated diffusion rate (Coble, 1961; Radonjić & Srdić, 1997).

Of the theories that were proposed to explain the mechanisms responsible for additive-enhanced densification in MgO-doped alumina are:

(1) The second-phase theory which proposes when MgO is added to alumina as a solute, a second phase material ($MgAl_2O_4$) precipitates to the grain boundaries of alumina and pin the grain boundary mobility during the final stage of sintering, and hence preventing discontinuous grain growth (Coble, 1961; Coble, 1962; Jorgensen & Westbrook, 1964).

(2) Solute segregation theory: it proposes that the solute material segregates to the grain boundary and hinder discontinuous grain growth by a solute drag mechanism (Jorgensen, 1965; Jorgensen & Westbrook, 1964).

(3) solid-solution theory: which proposes that when alumina is doped with MgO, the sintering rate is enhanced relative to the grain growth rate by the solute (Bennison & Harmer, 1983).

Johnson and Coble (1978) tested the aforementioned theories to determine if second-phase precipitation, calcium segregation or solid-solution is necessary for densification enhancement in doped alumina. They concluded that the enhanced densification of MgO-doped alumina cannot be explained neither by the second-phase pinning mechanism nor by the solute drag mechanism. Instead the solid-solution theory based on the alteration of grain growth and pore removal kinetics is a more reasonable explanation. Furthermore, grain boundary mobility was controlled by solid solution mechanism and it was dependent on the MgO concentration in the alumina-MgO solid solution (Greskovich & Brewer, 2001). Bennison and Harmer (1983) explained the effect of MgO on the grain boundary mobility and grain growth by the solute drag effect caused by the segregation of MgO to the grain boundaries (Bennison & Harmer, 1983).

From this literature, one can conclude that despite the vast number of studies, the influence of MgO on the densification process of alumina was not yet unequivocally demonstrated.

2.1.2 Titanium Oxide

The influence of titanium oxide or titania (TiO_2) on the densification and microstructural evolution of alumina is well-documented. Unlike MgO, almost all of the published articles agree on the role of TiO_2 as a grain growth promoter. Significant attention was given to the effect of TiO_2 on the microstructural evolution of alumina in the presence of liquid-phase-forming impurities, such as CaO and SiO_2. It is generally believed that AGG is caused by the presence of liquid-phase-forming impurities. These impurities segregate to the grain boundaries and their accumulation increase with grain size, until grain size reaches a critical value, impurity concentration exceeds the solubility limit in alumina which result in intergranular liquid film appearance. This liquid film was suggested to trigger AGG by increasing grain boundary mobility (Bae & Baik, 1997; Bae & Baik, 1993).

Bagley et al. (1970) found that the densification rate of alumina was accelerated by additions of TiO_2. The densification rate increased approximately exponentially with increasing the TiO_2 content up to a certain solute percentage, after which the densification rate levelled off or decreased slightly. This percentage is believed to be the solubility limit of TiO_2 in alumina, and the solubility limit increased with decreasing alumina particles size. The diffusion constant increased with increasing TiO_2 content until maximum value, after which the diffusion rate decreased. The decrease in the diffusion rate is believed to be due to the formation of second phase.

Kebbede et al. (1997) studied the influence of TiO_2 doping on tailoring the microstructure of alumina for improved mechanical properties. According to this study, anisotropic grains in equiaxed matrix improve the mechanical performance of ceramic materials. They found that TiO_2-doped samples developed a much larger grains relative to undoped alumina, whereas, alumina codoped with TiO_2 and SiO_2 resulted in an anisotropic microstructure containing platelets of alumina with large aspect ratio. This anisotropic microstructure caused by cooperative action of both dopants: SiO_2 and TiO_2. Moreover, anisotropic microstructure increased the fracture toughness of alumina. The authors also suggested that the microstructure of alumina can be tailored by varying the TiO_2 doping content to produce controlled volume fraction of platelet grains.

Min et al. (2000) found that TiO_2-doped alumina developed large grains, but without AGG. But, when alumina was codoped with TiO_2 and SiO_2, abnormal anisotropic grain growth was observed. Codoped alumina developed platelike grains 800 μm in length and 100 μm in thickness in otherwise fine matrix. They explained the anisotropic grain growth by the liquid phase formation during the sintering process. Aluminium titanate second phase (Al_2TiO_5) was detected using XRD analysis. Scanning electron microscope (SEM) micrographs showed localized regions with grain size smaller than the average grain size (Figure 2.1). The slow grain growth was believed to be caused by the precipitation of the second phase material at these regions of small grain size.

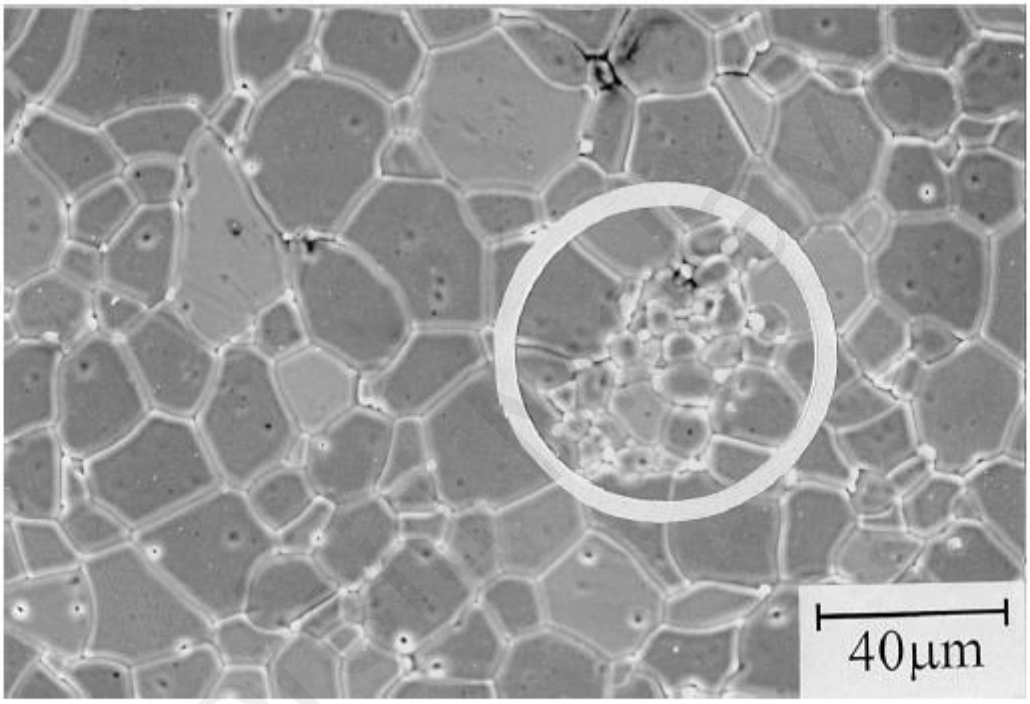

Figure 2.1: SEM micrograph of TiO_2-doped alumina (Min et al., 2000).

Furthermore, Horn and Messing (1995) observed the same anisotropic grain growth in TiO_2-doped alumina, but claimed that silicon is not a prerequisite for anisotropic grain growth in alumina. Miaofang et al. (2003) observed bilevel solubility in TiO_2-doped alumina. The two levels of solubility associated with equiaxed and anisotropic microstructure, and the high solubility level correspond to the anisotropic grains. The high solubility associated with anisotropic grains was explained by the presence of SiO_2 liquid phase at the intergranular regions which facilitated the incorporation of Ti^{3+} solute.

Mishra et al. (1996) found that TiO_2 enhanced the densification kinetics of alumina sintered using plasma activated sintering. Sylvie et al. (2006) also found that TiO_2 promoted the densification process of alumina by anisotropic grain growth. They observed a densification peak in TiO_2-doped alumina and at high dopant concentrations, this densification peak shifts to lower temperatures corresponding to the transformation of the dopants from being segregated to the grain boundaries to the precipitation of a second phase.

Zhang et al. (2010) studied the effect of TiO_2 doping on the densification of alumina and silica mixture. The mixture was activated using high energy ball milling. They found that small concentrations (< wt. 3%) of TiO_2 promoted anisotropic grain growth of mullite, whereas high concentration (> 5 wt. %) of TiO_2 suppressed the anisotropic grain growth resulting in better densification.

On the other hand, Bernardgranger and Guizard (2007) compared the densification path of undoped alumina, MgO-doped alumina and TiO_2-doped alumina. Samples were densified using HIP method. This study found that MgO doping resulted in a finer microstructure for a given density, whereas TiO_2 had no significant influence on the densification path and grain size of alumina. The sintering path of undoped alumina and TiO_2-doped alumina was similar.

The aforementioned studies almost agree on the role of TiO_2 as a densification and grain growth promoter in alumina, particularly in the presence of liquid-phase-forming impurities.

2.1.3 Yttrium Oxide

Yttrium oxide (Y_2O_3) positive effects on corrosion resistance (Gall et al., 1995) and creep resistance of alumina (Cho et al., 1997) are well documented. It is also widely accepted that yttrium induce a detrimental effect on the densification rate of alumina (Sato & Carry, 1996).

In 1968 US patent, Y_2O_3 was first described as a beneficial dopant for alumina. The combination of Y_2O_3 and MgO, 0.05 % Y_2O_3 plus 0.05 % MgO, was described as outstanding. With this combination, highly-dense alumina compacts with excellent mechanical properties and 2 – 3 µm average grain size were achieved (Lartigue et al., 2002). Later in mid 1970s, in another US patent, Y_2O_3 concentration in the range of 0.05 – 0.5 % by weight was proposed to be the optimum for alumina as far as densification is concerned (Korinek et al., 2002). Delaunay et al. (1980) also found that minor Y_2O_3 increased the densification rate of alumina which was explained by the increased diffusion rate and vacancy movement.

Later though, recent studies contradict the previous studies and found that yttrium induced a detrimental effect on the densification rate of alumina. Nanni et al. (1976) found that the activation energy for sintering of Y_2O_3-doped alumina was higher relative to undoped alumina. The increase in the activation energy was attributed to the segregation of Y_2O_3 to the grain boundaries of alumina. Chen and Chen (1996) studied the influence of number of dopants on the grain boundary mobility of alumina. They found that 1.0 % Y slowed down grain boundary mobility the most, whereas 0.1% Mg enhanced grain boundary mobility the most. Fang et al. (1997) further supported this conclusion and reported densification decrement by a factor of 11 in Y_2O_3-doped alumina. The observed densification slowness was explained by grain boundary diffusivity reduction. This study also found that Y_2O_3 hindered grain growth but at the penalty of slow densification rate.

To understand the contradictory results of the early studies on the effect of Y_2O_3 on the sintering of alumina, Sato and Carry (1993) investigated the sintering behavior and microstructural evolution of alumina doped with various amounts of Y_2O_3. Alumina powder was codoped with Y_2O_3 (225 and 775 ppm), and MgO (500 ppm). They found that the main densification rate peak for Y_2O_3-doped alumina was shifted to a higher temperature. There was an increase in the apparent activation energy of the intermediate stage of sintering which increased with Y_2O_3 content. In addition, Y_2O_3-doped alumina exhibited an abnormal densification rate peak at a temperature that decreased with increasing Y_2O_3 content (Figure 2.2). This abnormal peak corresponds to yttrium transition from grain boundary segregation to precipitation of yttrium aluminum garnet (YAG). At this densification rate peak, yttrium grain boundary segregation near the saturation limit increased the densification rate, and the abnormal peak shifts to a lower temperature as the yttrium content increase.

Of the more recent studies on the densification of Y_2O_3-doped alumina, Nakagawa et al. (2007) investigated the effect of Y_2O_3 doping on the oxygen grain boundary diffusion in alumina. They found that Y_2O_3 doping hindered the oxygen grain boundary diffusion by 10 times relative to the undoped alumina. Other studies found that Y_2O_3 significantly retarded the densification process which was inferred from the high activation energy of densification for Y_2O_3-doped alumina relative to undoped alumina and MgO-doped alumina (Galusek et al., 2012; Maca et al., 2014). The observed densification retardation in Y_2O_3-doped alumina was attributed to the limited solubility of Y_2O_3 in alumina which causes yttrium cations to segregate to the grain boundaries of alumina (Maca et al., 2014).

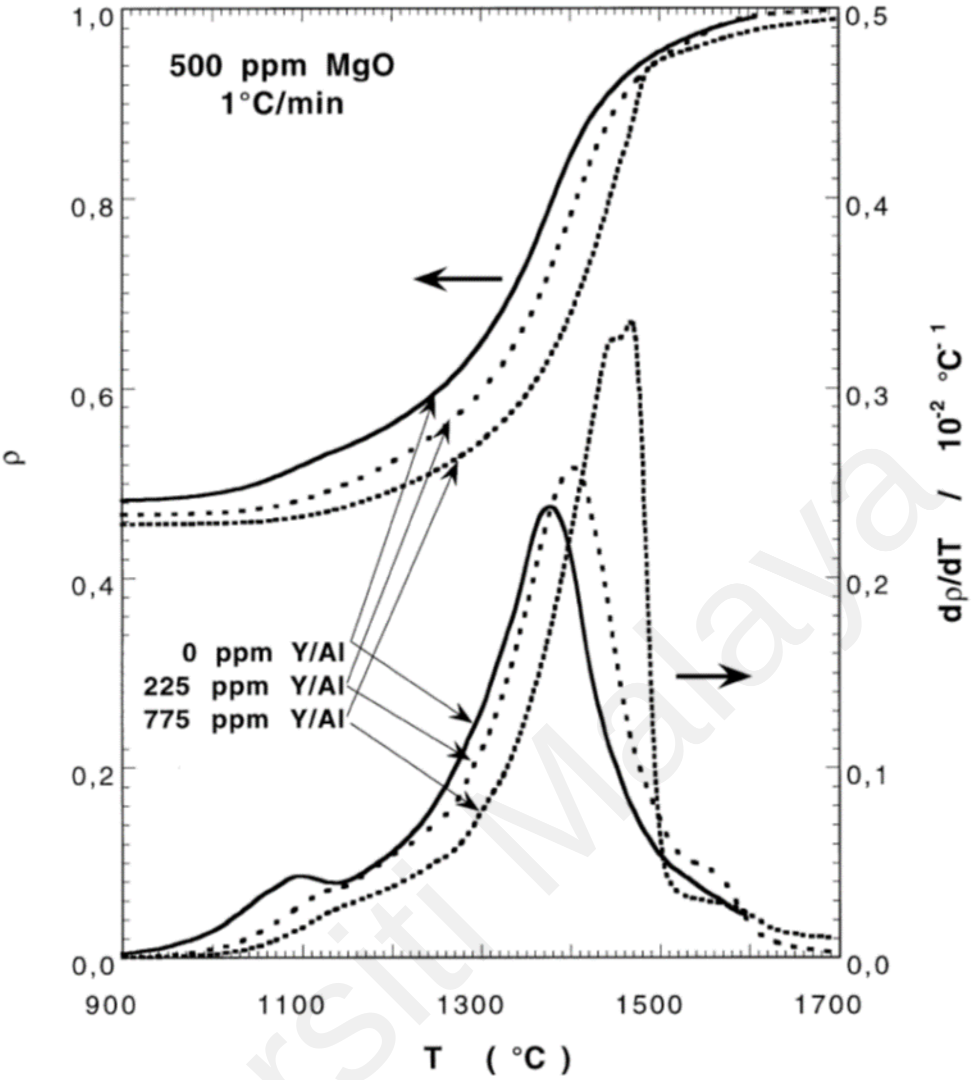

Figure 2.2: Sintering behaviour of Y_2O_3-doped alumina: an abnormal densification rate peak is observed (Korinek et al., 2002).

In a later study, Galusek et al. (2015) supported this conclusion and reported that Y_2O_3 retarded the densification process of alumina and hindered grain growth. The rise in the activation energy of sintering was attributed to the segregation of Y_2O_3 to the interfacial regions of the solvent material. The segregation of large yttrium cations slowed down the mobility of Al^{3+} and O^{2-} ions and hence resulted in limited grain boundary mobility (Bodišová et al., 2015; Maca et al., 2014).

2.1.4 Manganese Oxides

Manganese as a densification enhancing additive for different ceramics was the subject of number of studies. There is a good agreement on the positive effect of manganese on the densification of a number of ceramic materials including zirconia (Clavel et al., 2008; Ramesh et al., 2011; S. Ramesh et al., 2008; Zhang et al., 2009), ceria (Zhang et al., 2002; Zhang et al., 2003), and hydroxyapatite (Ramesh et al., 2016).

The densification and mechanical properties of manganese-doped zirconia were extensively studied. According to Li et al. (2017) yttria-stabilized zirconia (YSZ) showed reduced effective densification temperature by around 200 °C as a result of doping with manganese. The grain boundary diffusion activation energy decreased from 219.9 kJ/mol for YSZ to 103.4 kJ/mol for YSZ doped with 3-mol% manganese. This effect was explained by the concurrent reduction in the activation energies and change in the interfacial energies as a result of manganese segregation to the grain boundaries. An interesting desintering (desintering is the decrease in density as the sinering process continues) phenomenon was observed after prolonged sintering for manganese-doped YSZ. The desintering was explained by the evaporation of manganese at high temperatures. Zhang et al. (2009) also found that the presence of manganese in YSZ enhanced the densification process and promoted grain growth, which was explained by the reduction in apparent activation energy of manganese-doped YSZ.

Zhou et al. (2011) also reported improved densification, hardness, and bending strength of manganese-doped YSZ in comparison to undoped YSZ. Relative density and mechanical properties increased with increasing manganese content up to 3.0 wt. %. The enhancement in mechanical performance was attributed to the enhanced density and refinement in grain size. Chong et al. (2016) also found that manganese presence in YSZ promoted densification and grain growth. 3.0 wt. % manganese concentration was found to yield the optimum densification rate and optimum mechanical properties.

Addition of manganese (particularly greater than 0.3 wt. % of MnO_2) aided densification of yttria-tetragonal zirconia polycrystals (Y-TZP) and improved matrix stiffness and hardness of low-temperature sintered Y-TZP (Ramesh et al., 2008). In another related study, Ramesh et al. (2011) studied the effect of manganese and short isothermal dwell time (12 minutes) on the densification and mechanical performance of Y-TZP. This study found that 1.0 wt. % manganese addition was beneficial in enhancing the densification and the mechanical properties of Y-TZP. 1.0 wt. % manganese-doped Y-TZP reached 95% relative density at approximately 100 °C lower than the temperature needed for the undoped samples to reach the same density. The enhanced densification in short sintering time was attributed to the formation of transient liquid phase during sintering of manganese-doped samples.

In other related studies, it was found that manganese doping content of 0.3 wt. % was beneficial in enhancing the densification process of Y-TZP and 1.0 wt. % manganese content resulted in improved hardness and fracture toughness of Y-TZP (Meenaloshini et al., 2011; Ramesh et al., 2013). Kwa et al. (2015) found that 0.5 wt. % manganese concentration combined with short sintering time improved the mechanical properties (hardness, young's modulus, and fracture toughness) of Y-TZP. 1.0 wt. % manganese concentration, however, did not affect the mechanical performance of Y-TZP.

Ng et al. (2016) investigated the effect of various manganese doping concentrations in ceria-doped scandia stabilized zirconia. This study found that manganese concentration of 0.5 wt. % suppressed grain growth and manganese concentration of 5.0 wt. % had detrimental effect on the densification of ceria-doped scandia stabilized zirconia as it resulted in exaggerated grain growth (> 18 µm). Furthermore, 1.0 wt. % manganese content did not affect the mechanical performance.

The densification of ceria ceramics doped with manganese was studied by many researchers. Castro et al. fast fired ceria doped with manganese and observed a high densification in comparison to undoped samples. This enhanced densification was attributed to the formation of solid solution of manganese ions and ceria atoms, and to the segregation of manganese atoms onto particles surface (Pereira et al., 2005).

Tianshu et al. (2001); Zhang et al. (2002) studied the densification behavior of manganese-doped ceria. They reported that manganese increased grain boundary mobility and reduced the effective sintering temperature. The reduction in sintering temperature was over 200 °C for dopants content over 1 %. Manganese-doped ceria samples reached full densification (99 % relative density) at 1300 °C, whereas undoped ceria could only achieved 96 % relative density at sintering temperature of 1525 °C. Wu et al. (2015) studied the behaviour of manganese doping in nanocrystalline ceria. They reported that manganese segregated to both interfaces and grain boundaries with more segregation to the grain boundaries than to the surfaces. Manganese segregation caused significant reduction on the grain boundary energy from 0.87 J m^{-2} to 0.30 J m^{-2}. Grain boundary excess energy is one of the main driving forces for coarsening. The tendency of manganese segregation was determined using atomistic simulations and later confirmed using microcalorimetric energy measurements.

Hydroxyapatite (HA) is another ceramic material that exhibited enhanced densification with manganese doping. Ramesh et al. (2016) studied the effect of manganese on the sinterability and mechanical properties of HA. Manganese was added to the alumina powder in the form of MnO_2. This study found that HA doped with manganese percentage less than 0.5 wt. % exhibited better mechanical properties than undoped HA, and manganese-doped HA achieved marginally better relative density than undoped HA when sintered at 1150 °C. 0.05 wt. % manganese was found to be the best additive percentage for improved mechanical properties: hardness, fracture toughness, and Young's modulus. Hardness increased with density to a certain limit after which the hardness decreased. This decrement was attributed to grain growth at higher sintering temperature.

The effect of manganese as a densification enhancing dopant on sol-gel derived biphasic calcium phosphate was studied by Sopyan et al. (2011), and they reported an increase in crystallinity and densification with manganese content. The increase in crystallinity was explained by the progressive particle diffusion. Additionally, this study found that manganese addition reduced the effective sintering temperature of HA.

Acchar and Ramalho (2008) investigated the effectiveness 5 wt. % manganese addition on the sintering process, physical properties, and microstructural evolution of tricalcium phosphate (TCP). It was found that manganese lowered the onset temperature of densification and enhanced the final density of TCP. Manganese-enhanced densification was explained by the formation of liquid phase between manganese and TCP.

Although manganese was deemed an effective densification enhancing sintering additive, studies on manganese-doped alumina are scarce. In 1965 and 1968, Keski and Cutler (Keski & Cutler, 1968; 1965) showed that the densification rate of alumina improved by manganese addition up to 0.3 %. Other studies found that high concentration of alumina (3.0 wt. %) enhanced densification and hardness of alumina at low and high sintering temperatures (1250 – 1650 °C) (Erkalfa et al., 1995; Erkalfa et al., 1995). No significant final density variations were obtained from previous studies in which manganese-doped alumina samples were sintered at temperatures exceeding 1500 °C. Both undoped and manganese-doped samples reached final densities in the range of 98 – 99 %. Furthermore, inhomogeneous microstructure or exaggerated grain growth were observed in manganese-doped alumina at certain manganese levels (Erkalfa et al., 1995; Sathiyakumar & Gnanam, 2002). To the best of our knowledge, there is no published study concerning the low to moderate temperature (1300 -1500 °C) densification of alumina doped with low manganese concentrations (0.1 – 1.0 wt. %). This study shows that low manganese concentrations can enhance the densification and hinder grain growth of alumina at moderate sintering temperatures.

2.2 Microwave Sintering

Over the last decades, microwave heating has been widely studied as a rapid heating technique and as a potential substitute for conventional furnaces. Microwave heating has become an established method for many industrial applications including food processing, organic chemistry, pharmaceutical industry, food processing, etc. (Venkatesh & Raghavan, 2004; Vongpradubchai & Rattanadecho, 2009; Zong et al., 2003). These applications rely on electromagnetic energy absorption in water or organic materials at relatively low temperatures. Microwave heating in high temperature applications, such as powder metallurgy, is still under research and development and it is expected to mature in the near future.

2.2.1 Heating mechanisms in conventional sintering and microwave sintering

A key feature in microwave sintering is the volumetric energy absorption in many materials compared to its conventional counterpart in which energy is transferred by conduction, convection and radiation. In microwave sintering, the material being sintered couples with and transform the electromagnetic energy into heat. This results in a rapid volumetric heating of the material. Because of this volumetric heating, the power produced by microwaves can be fully utilized to heat the product with minimum energy waste which enables high heating rates to be applied. Because heat is transferred by conduction, convection, and radiation in conventional sintering, significant portion of the energy is wasted in heating the furnace itself rather than heating the product (Bykov et al., 2010).

In conventional heating, a temperature gradient develops across the material from the surface to the inside and in microwave heating the temperature gradient develops from the inside to the surface. The temperature gradient in microwave sintering, however, can be solved by the use of a susceptor that can provide uniform heat distribution across the specimen because microwaves heat the specimen volumetrically and the radiative heat provided by the susceptor minimizes the surface heat loss (Clark & Sutton, 1996). When a susceptor is used in microwave sintering, the process is referred to as "hybrid microwave sintering" (Jeremy Croquesel et al., 2016). Figure 2.3 shows temperature profiles for conventional sintering, microwave sintering, and hybrid microwave sintering. Figure 2.4 shows two-way hybrid microwave heating with susceptors.

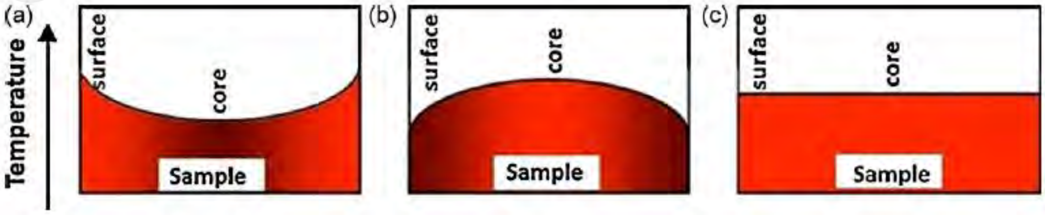

Figure 2.3: Samples' temperature profile in (a) conventional sintering, (b) microwave sintering, (c) hybrid microwave sintering (Oghbaei & Mirzaee, 2010).

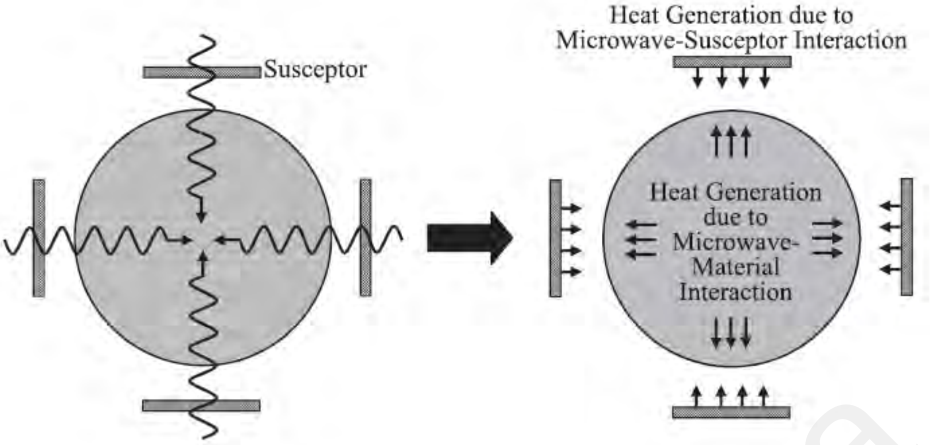

Figure 2.4: Two-way hybrid microwave heating with susceptors (Bhattacharya & Basak, 2016).

During microwaves interaction, a material can reflect, absorb and/or transmit microwaves and this depends upon the dielectric loss factor of the material. Dielectric loss factor determines how good a material can couple with microwaves. Based on dielectric loss factor, materials can be classified as: (1) transparent: a low loss insulator, (2) opaque: conductor, (3) absorbing: high loss insulator. At room temperature, most ceramic oxides are low loss insulators and tend to heat up very slowly in microwave field. Alumina has a loss factor of tan δ ~ 0.045% at room temperature (Peng et al., 2013) at microwave frequency of 2.45 GHz. Alumina is a typical example of low loss ceramics. Generally, the dielectric loss factor tends to increase exponentially with increasing temperature (Zhao et al., 2000). Figure 2.5 shows a schematic for microwaves interaction with the three types of material: transparent, opaque, and absorber.

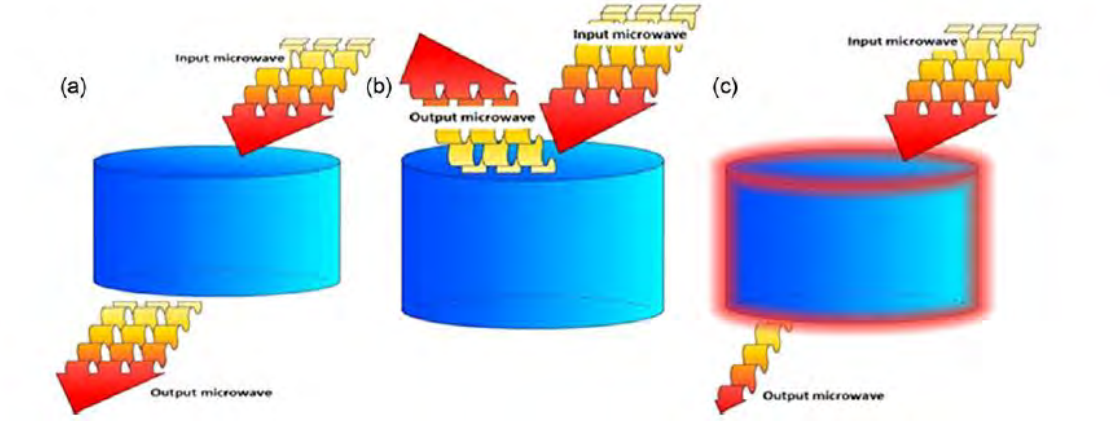

Figure 2.5: Microwave interaction with three type of materials (a) transparent, (b) opaque, (c) absorber (Oghbaei & Mirzaee, 2010).

The low loss of alumina at low temperatures significantly reduces its ability to couple with microwaves. But this problem can be overcame by using high dielectric loss factor susceptor. The use of susceptor enables heating low loss specimen to a temperature at which it shows significant coupling with microwaves. SiC is commonly used as a susceptor in microwave heating due to its high loss factor at room temperature and its excellent refractory properties (Zhao et al., 2000). The dielectric loss factor of alumina also depends on the doping elements such as magnesium (Mollá et al., 1996) and yttrium (Song et al., 2007) or other impurities present in alumina powder.

Numerous studies reported various advantages for microwave sintering over conventional sintering, these advantages include: (1) shortened sintering time (2) reduced energy consumption, (3) lower processing cost, (4) enhanced diffusion process, (5) lower effective sintering temperature, (6) rapid volumetric heating, (7) enhanced physical and mechanical properties.

Economically, microwave sintering has clear advantages with respect to energy consumption, which arises from the shortened cycle time (Thuault et al., 2014; Xie et al., 1998), rapid volumetric heating, and lower effective sintering temperatures (Oghbaei & Mirzaee, 2010; C. Zhao et al., 2000). A study claimed that microwave processing reduces the sintering time by a factor of more than ten (Agrawal, 2006). On the prospect of microwave sintering applications, according Monaco et al. (2015), the reduction in sintering time enabled by microwave sintering is significant in dentistry and "could allow the introduction of zirconia in chair-side treatments, if used as a monolithic material".

2.2.2 Material's dielectric properties effects

The effect of the material dielectric properties on the densification process under microwave was studied by Wang et al. (2006). Three ceramic materials: ZnO, 3-YSZ, and Al_2O_3, with different dielectric properties were tested. The study found that the material with the greatest microwave absorption (ZnO) showed the highest densification enhancement under microwaves. 3-YSZ, a moderate microwave absorber, showed a moderate densification enhancement. Al_2O_3, a poor microwave absorber, showed insignificant densification enhancement. Binner et al. (2007) supported this conclusion by claiming that the extent of the so-called "microwave effect" depends on the material's dielectric loss; the higher the dielectric loss the more significant the effect. Zuo et al. (2014) conducted a comparative analytical study to compare the apparent activation energy of α-alumina and ZnO under conventional heating conditions and microwave heating. The apparent activation energy for $\alpha\text{-}Al_2O_3$ under microwave heating condition was lower than that of $\alpha\text{-}Al_2O_3$ under conventional heating. The apparent activation energy for ZnO was higher under microwave field. It concluded that microwave filed could play a role in changing the diffusion mechanism depending on the material dielectric properties.

The dielectric properties of a material is effected by dopants or impurities present in the material. For instance, Song et al. (2007) found that the dielectric loss of alumina was increased by doping with yttria. The dielectric loss increased from 8.4×10^{-5} to 2.2×10^{-4}. This increase in the dielectric loss was attributed to the precipitation of a second phase $Al_5Y_3O_{12}$ which results from the limited solubility of yttria in the corundum lattice. In another study, it was shown that the dielectric loss factor of polycrystalline alumina was significantly reduced by doping alumina with titania. The titania-doped alumina exhibited dielectric loss factor approaching that of single crystalline alumina (sapphire) (Alford & Penn, 1996).

2.2.3 Effects of microwaves on the sintering temperature

Reduction in the effective sintering temperature under microwaves was reported for different ceramic materials. For a given density to be achieved in partially stabilized zirconia, hybrid microwave sintering reduced the required temperature by 80 – 100 °C relative to the temperature needed for conventional sintering to achieve the same density (Wroe & Rowley, 1996). Wang et al. (2006) observed an enhanced densification and higher relative density at a given temperature for ZnO, 3-YSZ and Al_2O_3 using hybrid microwave-sintering. zirconia-toughened alumina also achieved higher relative density when sintered using microwave in comparison to conventional sintering (Manshor et al., 2017). In another study, Monaco et al. (2015) reported that microwave enabled a reduction in sintering temperature of commercial zirconia (Y-TZP) from 1480 °C to 1200 °C. Ramesh et al. (2018) found that the microwave-enhanced densification for YSZ was at its peak at low sintering temperature of 1200 °C. However, as the sintering temperature increased to 1500 °C, microwave-enhanced densification was insignificant. Nano-sized titanium nitride also showed enhanced densification at using microwave sintering (Demirskyi et al., 2013).

Alumina in its pure form or doped with various transitional metal oxides was the subject of number of studies concerning microwave sintering. The densification of coarse and nano-sized mixture alumina powder was enhanced using microwaves (Liu et al., 2012). The densification onset temperature of alumina was lower during microwave sintering relative to conventional sintering (Croquesel et al., 2016; Croquesel et al, 2017), and apparent activation energy reduced by microwave heating in comparison to conventional sintering (Zuo et al., 2014). Microwaves lowered the phase transformation temperatures for γ phase alumina (Bykov et al., 2010; Croquesel et al., 2016; Rybakov et al., 2008). A mix of doped α-alumina and γ-alumina were sintered in conventional furnace and in multimode microwave furnace. Samples sintered under microwave field reached 95 % theoretical density at 1350 °C, whereas conventionally sintered samples achieved the same density at 1600 °C (Brosnan et al., 2003). Ultrafine commercial alumina was sintered using microwaves and conventional furnace. It was reported that microwaves enhanced the densification relative to conventional sintering which was explained by high heating rates and effective particle packing during microwave sintering (Golestani et al., 2011).

Fang et al. (2004) reported that microwave enhanced the densification of alumina compacts without pre-sintering heat treatment, but when the powder was subjected to pre-sintering heat treatment, the microwave-enhanced densification gradually decreased and eventually vanished as the heat treatment increased. Transparent alumina was prepared using microwave sintering by Cheng et al. (2002). They reported that microwave enabled fabrication of transparent alumina at sintering temperature lower than that needed by conventional sintering. Furthermore, they found that microwave significantly increased the conversion rate of polycrystalline alumina to single crystalline alumina. Wang et al. (2008) studied the effect of microwave sintering on the densification of sol-gel-derived alumina film. Their results supported the existence of the so-called “microwave effect” and they found that microwaves enhanced the densification and phase transformation of sol-gel-derived alumina films and the microwave-enhanced densification increased with increasing microwave power from 600 W to 1000 W.

On the other hand, in a recent novel study using single mode microwave furnace, Croquesel et al. (2017) studied the effect of microwaves on the densification process of MgO-doped alumina. Densification of samples sintered using microwaves started at lower temperature for doped and undoped samples, however, this effect vanished at the later stages of sintering. Before that, Xie et al. (1998) also observed an enhanced densification process in microwave-sintered samples at low sintering temperatures (from 1000 to 1400 °C). But this microwave-enhanced densification vanished as the sintering temperature increased to 1400 °C resulting identical relative densities (99.7 %) for microwave-sintered and conventionally-sintered alumina.

2.2.4 Microwaves effects on grain growth

Grain refinement was reported for many ceramic oxides sintered using microwaves. Studies on grain size/density trajectory (sintering path) of nano-powder titanium nitride (Demirskyi et al., 2013) and zirconia-toughened alumina (Manshor et al., 2017) showed that microwave-sintered samples followed different sintering path than that of conventionally sintered samples. That is, microwave-sintered samples yielded finer average grain size for a given density than the average grain size of conventionally-sintered samples. While other studies reported no significant difference in the grain size of microwave-sintered and conventionally-sintered compacts, this includes a recent study by Ramesh et al. (2018) which reported no significant difference in grain size between microwave-sintered YSZ and conventionally-sintered YSZ.

Concerning alumina, numerous studies claimed that microwave sintering did not affect the grain growth in alumina. For instance, Brosnan et al. (2003); Xie et al. (1998); Zuo et al. (2015) reported that grain size grew at similar rates at higher densities despite the difference in sintering temperatures and grain size/density trajectory of alumina was similar for both heating methods: microwave sintering and conventional sintering. Furthermore, Xie et al. (1998) even found that during microwave sintering of alumina, with holding time, grains grew at faster rate than the rate observed during conventional sintering (Figure 2.6). On the other hand, Golestani-fard et al. (2011) studied the densification of ultrafine commercial alumina and claimed that microwave sintering was beneficial in obtaining finer microstructure in comparison to conventional sintering.

2.2.5 Microwaves effects on the mechanical properties

Number of studies reported an improvement in the mechanical properties (hardness, fracture toughness, young's modulus, and flexural strength) in many ceramics when sintered in microwave furnace. Demirskyi et al. (2013) studied the microwave effect on the mechanical properties of nano-sized titanium nitride. An increase in hardness from 18 to 20 GPa and increase in fracture toughness from 2.9 to 3.4 MPa $m^{1/2}$ was reported. The microwave-enhanced mechanical properties were attributed to the finer grain size of microwave-sintered samples relative to conventionally-sintered samples. Zirconia-toughened alumina exhibited improved mechanical properties when sintered in microwave furnace. The improvement in the mechanical properties was explained by the enhanced densification, fine grain size, and homogeneous microstructure that was caused by microwave sintering (Manshor et al., 2017).

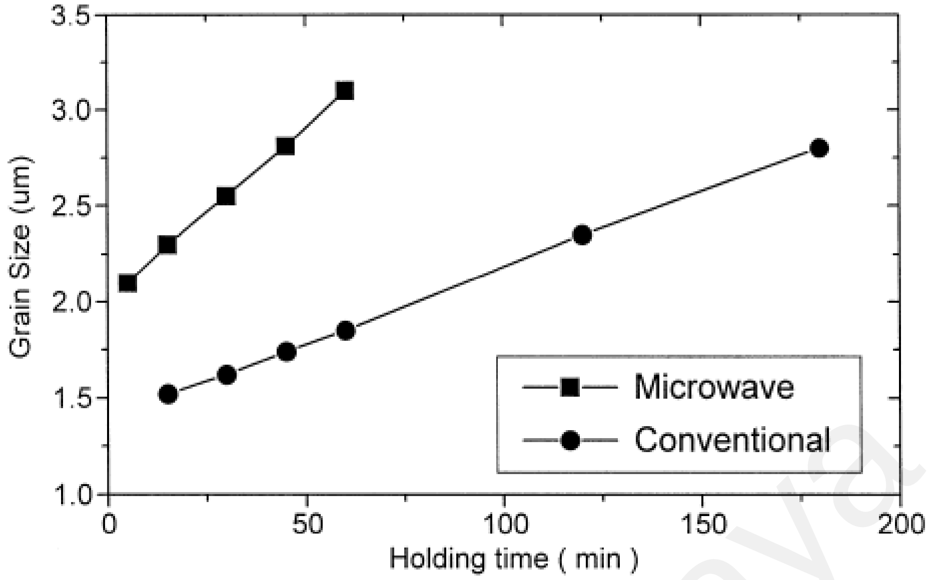

Figure 2.6: Grain growth with holding time at sintering temperature of 1500 °C (Xie et al., 1998).

Microwave sintering was beneficial in enhancing the densification and mechanical properties of YSZ at low sintering temperature of 1200 °C, however, as the sintering temperature increased to 1400 and 1500 °C, the densification and mechanical performance of YSZ were comparable for both sintering methods: microwave sintering and conventional sintering (Ramesh et al., 2018). Thuault et al. (2014) obtained significantly higher mechanical properties (hardness, Young's modulus, fracture toughness, and compressive strength) of HA using microwave sintering.

Liu et al. (2012) studied the effect of microwave sintering on the mechanical properties of a mix of coarse alumina powder and nano-sized alumina powder. They found that both microwave and nano-sized powder improved the mechanical properties of the samples. The improvement in the mechanical properties was attributed to the refinement in the grain size caused by microwave sintering. Golestani et al. (2011) reported a significant increase in the fracture toughness of alumina sintered using microwaves and it was explained by the microwave-enhanced densification which resulted from high heating rates and effective particle packing.

2.2.6 Effects of doping on the dielectric loss factor

As mentioned before, the material dielectric properties determine the way a material interact with microwaves. Dielectric properties are influenced by sintering additives and impurities. For instance, microwaves induced a palpable enhancement in the densification process and final density of alumina, and the addition of an amount of MgO causing the precipitation of secondary phase spinel ($MgAl_2O_4$) enhanced the densification even further (Zuo et al., 2014; Żymełka et al., 2013). This enhancement in the densification was attributed to the higher loss factor at the grain boundaries caused by the segregation of magnesium and impurities to the grain boundaries (Żymełka et al., 2013).

Titania-doped $MgAl_2O_4$ spinel material experienced an enhanced densification process – densification curve was shifted to lower temperatures – under microwave sintering in comparison to conventional Sintering. This result was attributed to species diffusivity enhancement provided by a specific coupling between the microwaves and Ti^{4+} and V''_{Mg} pair dipoles. Pure spinel materials did not affected by microwaves (Macaigne et al., 2016). The dielectric loss of alumina doped with yttria was studied by Song et al. (2007) and they found that yttria increased the dielectric loss of alumina, and therefore, decreased the sintering temperature of yttria-doped alumina. This increase in dielectric loss was attributed to the formation of secondary phase $Al_5Y_3O_{12}$ in yttria-doped alumina.

MgO in enhancing the densification process was observed in MgO-doped alumina sintered using microwaves. The presence of MgO was reported to improve the diffusion and densification process under microwave sintering. This enhancement was attributed to the improvement in the coupling capability of the material containing MgO due to the higher loss factor of segregated MgO and also to the increased concentration of the charges and vacancies (Zuo et al., 2013; Zuo et al., 2015; Żymełka et al., 2013). This conclusion, however, was contradicted by Croquesel et al. who found that MgO slowed down the densification process in alumina and this inhibition was exaggerated under microwave sintering. It is noteworthy that Croquesel et al. used a novel direct single mode microwave furnace with unique temperature monitoring system which enabled better temperature accuracy (Croquesel et al., 2017).

2.2.7 Effects of heating rate and holding time during microwave sintering

Effects of heating rates and isothermal dwell time during microwave sintering were studied by number of researchers. Rapid heating has reportedly resulted in improved densification and finer grain size for a given density. Rapid heating is feasible in microwave sintering because of the volumetric heating of the sample during microwave sintering. Volumetric heating minimizes temperature gradient across the sample, and thus mitigates differential sintering. In contrary, the temperature gradient that builds across the sample during high heating rate conventional sintering results in differential sintering across the sample (Menezes & Kiminami, 2008).

Gunnewiek and Kiminami (2014) studied the effect of microwave heating rate on the densification and grain growth of zinc oxide ceramics. Heating rates were varied between 50 – 100 °C/min. The study concluded heating rate had no effect on the final relative density, but high heating rates resulted in finer grain size. In addition, calculations showed that grain growth activation energy decreases with increase heating rate.

Yttria-stablized zirconia was studied using conventional sintering, two-step sintering and rapid heating microwave sintering. Two-step sintering produced the smallest grain size but with inhomogeneous grain distribution. Rapid heating microwave sintering produced small grain size in comparison to low rate microwave sintering and conventional sintering (Mazaheri et al., 2008). The effect of sintering temperature and holding time on the microstructure of Al_2O_3/Ti ceramic tool during microwave sintering was studied. At relatively lower temperatures, longer holding times were beneficial in obtaining higher densities. As the sintering temperature increased to higher than 1500 °C, longer holding times reduced the final density causing dedensification causing large cavities and open microstructure (Yin et al., 2016).

Many researcher tried to explain the reasons behind the enhanced microwave sintering. Wang et al. (2006) observed that the temperature gradient during microwave sintering, and the temperature gradient was found to be insignificant to explain the enhanced densification under microwaves. Hence, they asserted on the existence of the so-called "microwave effect". Furthermore, Binner et al. (2007) ruled out temperature gradient as a possible cause for microwave effect and concluded the genuine exist of the so-called "microwave effect". Other researchers attributed the microwave-enhanced densification to the ponderomotive force effect (Croquesel et al., 2016; Rybakov & Semenov, 1995; Wang et al., 2008).

2.3 Summary

Microwave sintering positive effect on the densification, microstructure and mechanical properties of ceramics has been reported, and yet, it has not been there are many controversial results in the literature. There are many parameters that can contribute to this controversy including but not limited to powder size, doping elements, temperature control accuracy, and heating rates.

Given the reported effects of manganese on the densification of many ceramic materials, and the lack of studies concerning manganese-doped alumina. The aim of this study is to investigate the effect of manganese addition on the densification, microstructural evolution and hardness of alumina. Additionally, certain dopants can affect the densification behavior during microwave sintering, and since manganese-doped alumina has never been sintered using microwave – to the best of our knowledge – microwave sintering will be compared with conventional sintering to explore possible effect of manganese during microwave sintering.

CHAPTER 3: METHODOLOGY

3.1 Green Body Preparation

Figure 3.1 illustrates the flow chart of the sample preparation and testing that were conducted in this research. Commercially available 99.9% pure Al_2O_3 (Kyoritsu, Japan) powder was used as a starting powder. Manganese dioxide (MnO_2) (BDH) powder was added to the alumina as a dopant. Alumina powder was mixed with predetermined amounts of manganese dioxide (0.1, 0.5 and 1.0 wt. %). Hereafter, for simplicity, each of these compositions will be referred to with a specific name as shown in Table 3.1. The mixture was homogenized using wet milling process (Bodišová et al., 2015; Lahiri et al., 2016) using attritor mill (Union Process, USA) for 30 minutes at 600 rpm with zirconia balls and ethanol as a milling medium. The mixture was dried in oven at 60 °C for 24 hours. The dried powder was then sieved through 212 µm to obtain flowing ready-to-press flowing powder. Desk-shaped samples (20 mm in diameter) and bar-shaped samples (4 mm, 13 mm and 32 mm in thickness, width, and length, respectively) were uniaxially pressed using manual hydraulic press machine. Pressed samples were subjected to cold isostatic pressing (CIP) (Riken, Seiki, Japan) under 200 MPa of pressure for 60 seconds. CIP induces uniform shrinkage and improve the densification by applying high pressure on all directions of the green body.

Table 3.1: Powder compositions used in this study.

Powder	Dopant content (MnO_2)
undoped	0
0.1-Mn	0.1 wt. %
0.5-Mn	0.5 wt. %
1.0-Mn	1.0 wt. %

3.2 Sintering

Sintering was carried out using conventional and microwave sintering methods. Conventional sintering was carried out in a box electrical furnace at four different temperatures: 1300, 1400, 1500, and 1600 °C. 10 °C /min heat-up and cooldown rate was applied with 2-hour dwell time.

Hybrid microwave sintering with a SiC susceptor was carried out in a multimode 2.45 GHz, 6 kW microwave furnace. Samples were sintered three different temperatures: 1300, 1400, and 1500 °C. Heat-up rate for microwave sintering was 30 °C /min with 5-minute dwell time. Then, the microwave power was turned off and the cooldown was uncontrolled until room temperature. Figure 3.2 shows conventional sintering and microwave sintering profiles.

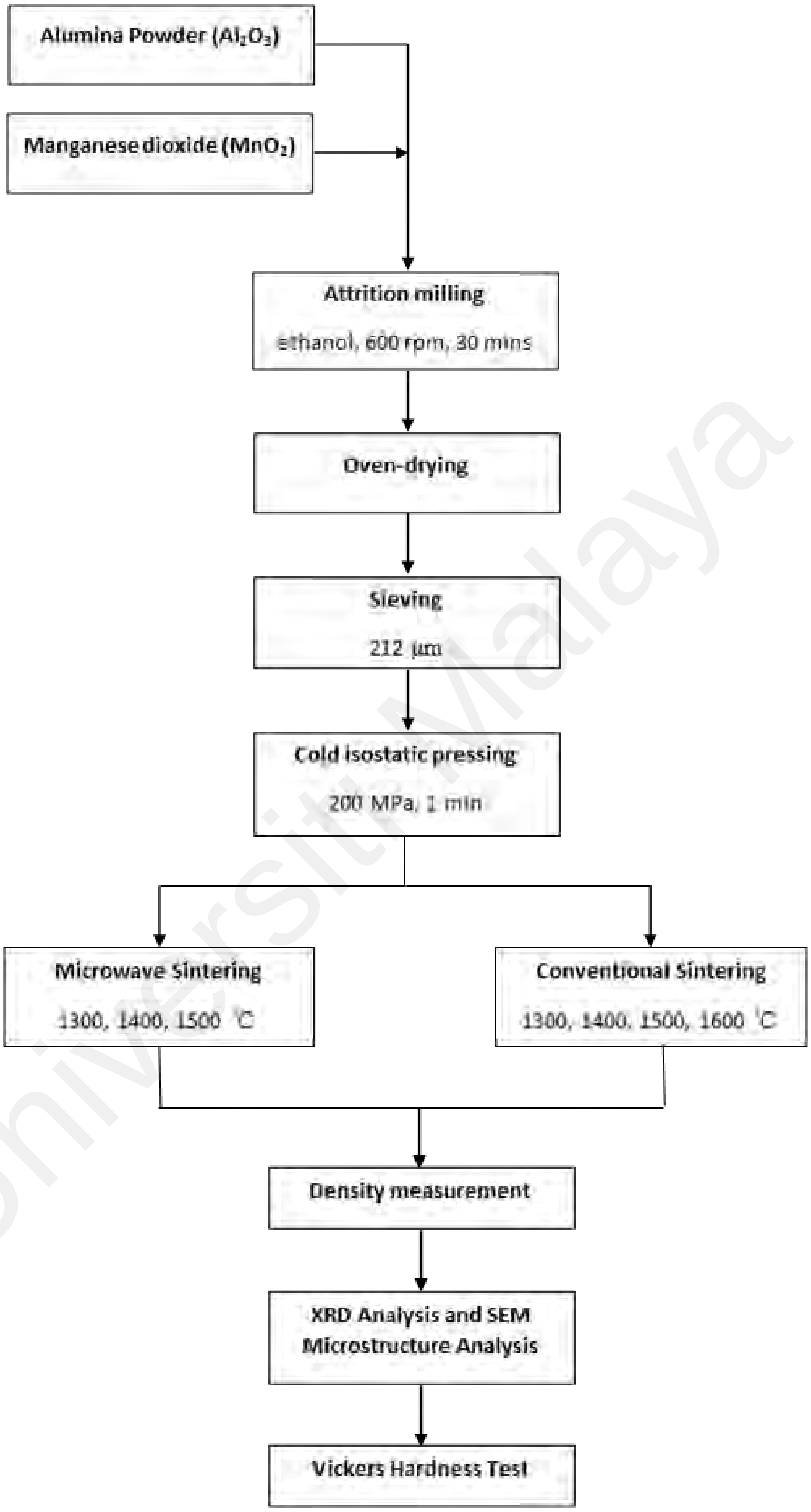

Figure 3.1: Research methodology flowchart.

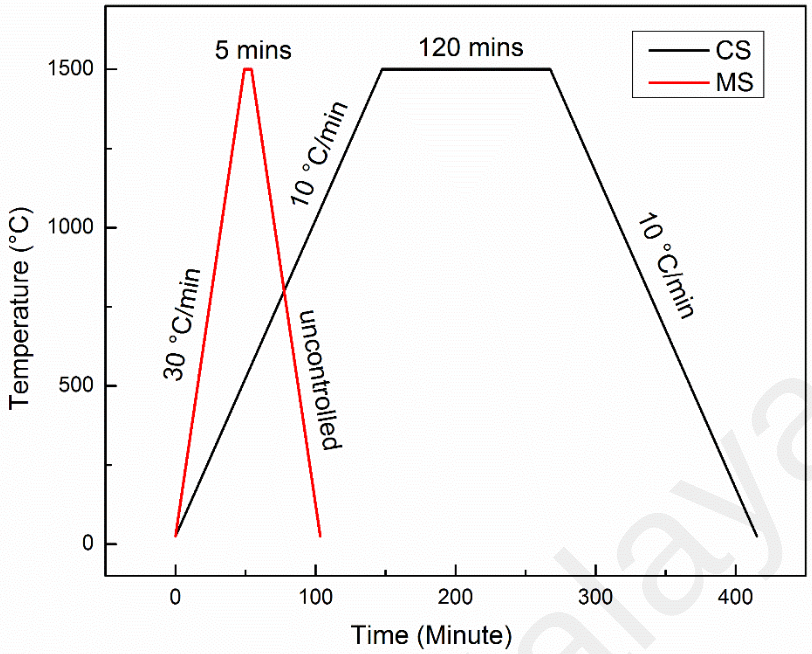

Figure 3.2: Conventional sintering and microwave sintering profiles.

3.3 Bulk Density Measurement

Bulk densities of the sintered samples were determined using water immersion method based on Archimedes' principle in accordance to the ASTM C373 - 18. Analytical balance with density measurement kit was used to record the weights of the samples in air, in water, and saturated weight after soaking in water. Samples' density were calculated using the following equation:

$$\rho_{bulk} = \frac{W_{air}}{W_{saturated} - W_{suspended}} \times \rho_{water} \qquad (2)$$

Where:

ρ_{bulk} = bulk density of the sample.

W_{air} = weight of the sample in air.

$W_{saturated}$ = weight of the sample after soaking in water.

$W_{suspended}$ = weight of the sample while immersed in water.

ρ_{water} = density of the distilled water which was taken to be: 0.997 g/cm^3.

The relative density was then calculated according to the following equation:

$$\boldsymbol{Relative\ density} = \frac{\boldsymbol{bulk\ density}}{\boldsymbol{theoretical\ density}} \times \mathbf{100} \qquad \mathbf{(3)}$$

The theoretical density of α-alumina was taken as 3.98 g cm^{-3} (Pillai et al., 2004).

3.4 Grinding and Polishing

Prior to conducting the XRD analysis, microstructure analysis, and Vickers Hardness test, disk-shaped compacts were ground and polished to obtain reflective surface. Grinding was done manually using silicon carbide (SiC) papers with different grades, starting from coarse (120) and finishing with fine grade paper (1200). After grinding, samples were manually polished using 6 µm and 1 µm diamond paste.

3.5 Phase Analysis

Sintered samples were analyzed using X-ray diffraction (XRD) (PANalytical Empyrean, Netherlands) to detect phases present after the sintering process. The X-Ray diffraction used in this study operates at 40 kV with Cu-Kα radiation source having a step mode of 0.02° 2θ step and a count time of 0.5s per step. Because alumina shows the highest peaks at 2θ angle in the range of 20° – 60°, the XRD test was done over the 2θ range of 20° – 60°. The obtained XRD patterns were compared with a standard reference patterns provided by the Joint Committee of Powder Diffraction Standard and the

International Centre for Diffraction Data (JCPDS and ICCD) to identify phases present in the samples.

3.6 Microstructure Analysis

The microstructure of the sintered compacts was examined using scanning electron microscopy (SEM). Prior to SEM scanning, samples were thermally etched at 50 °C lower than their corresponding sintering temperatures with heat up and cool down rate of 10 °C/min and 30-minute dwell time. The purpose of thermal etching is to reveal the microstructure.

Secondary electrons were used to take images at a voltage of 10.0 kV and magnification range 5000× to 500000×. Number of images were taken at various randomly selected spots (edge and center) throughout the samples. From the SEM micrographs, the average grain size was determined using the line intercept method (Mendelson, 1969) where a few lines were drawn on A4-size SEM micrographs. For each sample, not less than 250 grain boundary intercepts were counted. The number of grain boundaries intercepts were counted from which the average grain size was calculated according to equation 4 and 5:

$$D = 1.56\,L \qquad \textbf{(4)}$$

$$L = \frac{C}{MN} \qquad \textbf{(5)}$$

Where:

D = average grain size.

L = measured average interception length over the number of grains.

C = total length of test line.

M = magnification of photomicrograph.

N = number of intercepts.

3.7 Hardness Test

Hardness of the sintered samples were determined using Vickers Hardness tester (Mitutoyo AVK-C2, Japan) in accordance to the Standard Test Method for Vickers Indentation Hardness of Advanced Ceramics (ASTM C1327-15). Load value of 10 KgF was applied for 10 seconds.

To ensure the accuracy of the results, the hardness tester was calibrated prior to testing. The calibration was done using three certified hardness blocks. These blocks have hardness values ranging from low to high hardness to ensure accuracy at all hardness values.

Figure 3.3 shows a typical indentation shape formed by Vickers Hardness indenter. Generally, the typical result for Vickers indentation is a square with two diagonals having similar length ($d_1 = d_2$). The indentations process was repeated five time for every samples at different locations throughout the sample. The average diagonal value (D) was calculated from the five reading according to equation (6):

$$H_V = \frac{1.854P}{D^2} \tag{6}$$

Where:

H_V = Hardness Vickers number.

P = indentation load.

D = mean diagonal: $\frac{D1+D2}{2}$

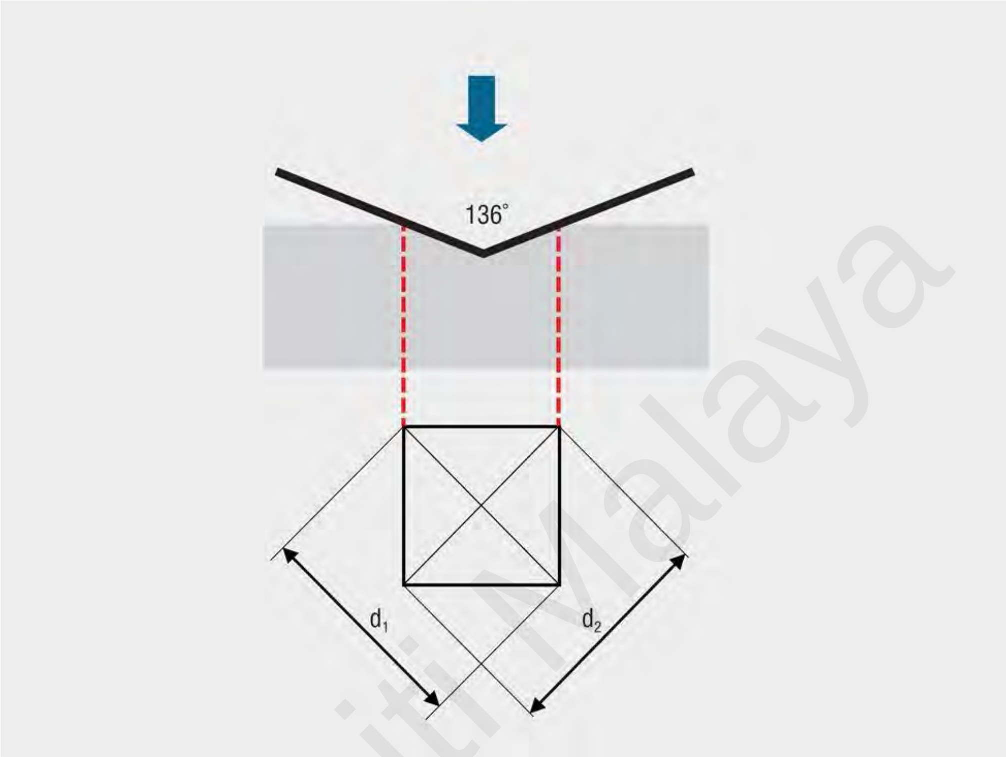

Figure 3.3: Typical Vickers Hardness indentation.

CHAPTER 4: RESULTS AND DISCUSSIONS

In this chapter, the finding of this study will be elaborated, discussed, and related to the available literature. This chapter is divided into two sections: 4.1 and 4.2. Section 4.1 concerns with the effect of the dopant, manganese, on the phase evolution, densification, microstructure, and mechanical properties of alumina. Section 4.2 compares the sintering behavior of conventionally-sintered and microwave-sintered samples.

4.1 Effect of Manganese Addition

4.1.1 Phase evolution

XRD analysis was performed for all sintered samples to reveal the phases developed during the sintering process. XRD was done at a two theta range from 20°- 60° because the major peaks of alumina appears in this range. Figure 4.1 shows XRD patterns of undoped and manganese-doped alumina sintered at 1600 °C.

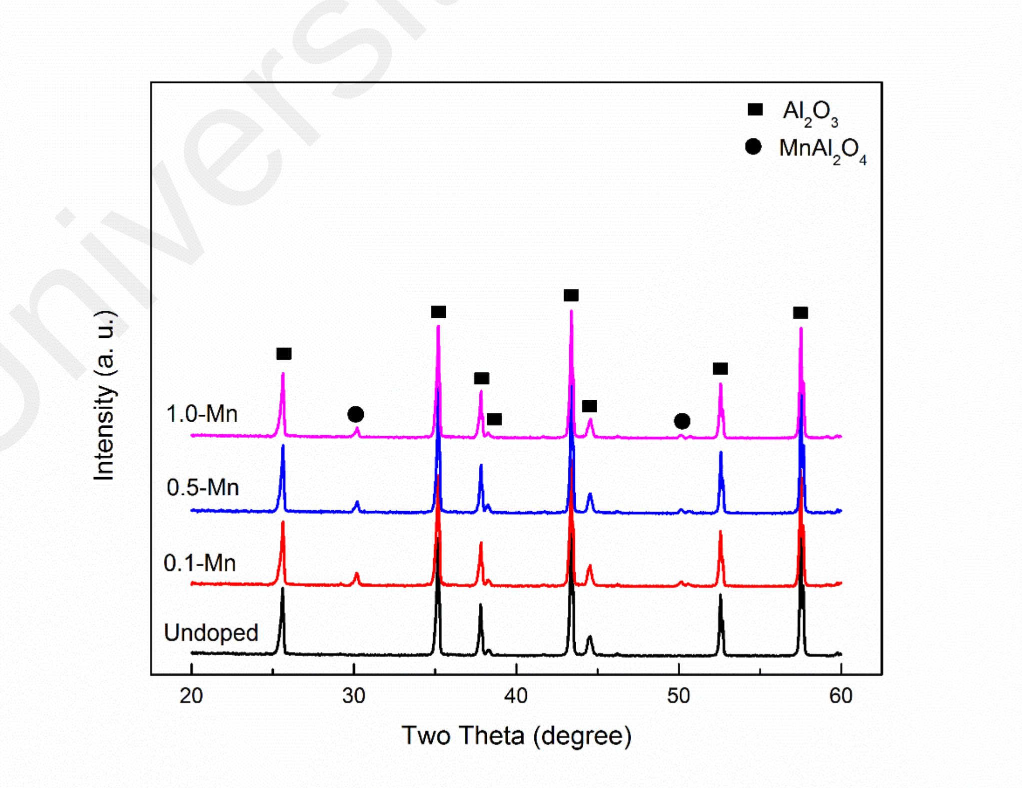

Figure 4.1: XRD patterns of different composition samples sintered at 1600 °C.

The XRD analysis revealed that all manganese-doped alumina sintered at different temperatures developed a spinel second phase ($MnAl_2O_4$). Second phase formation indicates a limited solubility of manganese in alumina. The valence difference between manganese and alumina leads to vacancies or interstitials creation in the corundum lattice. Because of the high energy involvement in this process no solubility was found for manganese in alumina (Roy & Coble, 1968). Keski and Cutler (1968) did not verify the existence of a second phase in manganese-doped alumina, but they assumed that the drop in the sintering rate that was observed in alumina samples containing > 0.3 wt. % manganese was due to the formation of a second phase. The XRD analysis in the present work, however, did not show variation in the second phase precipitation with increasing manganese content.

EDS was used to locate the second phase precipitation, but it could not detect the second phase presumably due to the small amount of second phase precipitates as the highest manganese content was 1.0 wt. %. Moreover, small percentages of manganese doping may have formed solid solution with alumina and therefore is difficult to detect. Figure 4.2 shows SEM micrograph with numbered spots in which EDS was performed. Figure 4.3 shows EDS spectra of the eight spots marked in Figure 4.2. Table 4.1 shows element concentrations detected by EDS analysis.

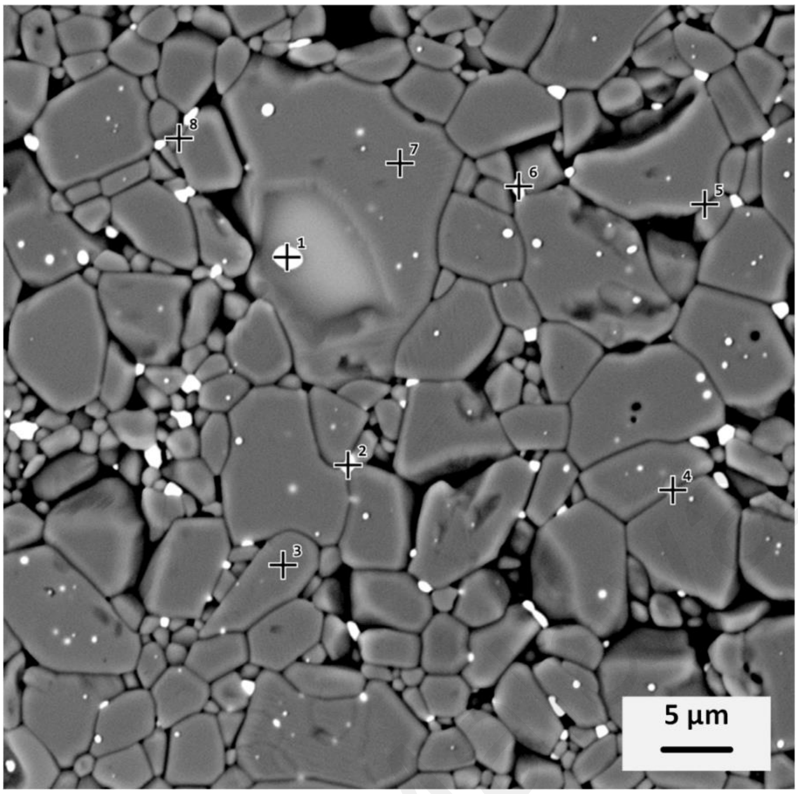

Figure 4.2: SEM micrographs shows eight marked spots in which EDS analysis was performed for 1 wt. % Mn-doped alumina sintered at 1600 °C.

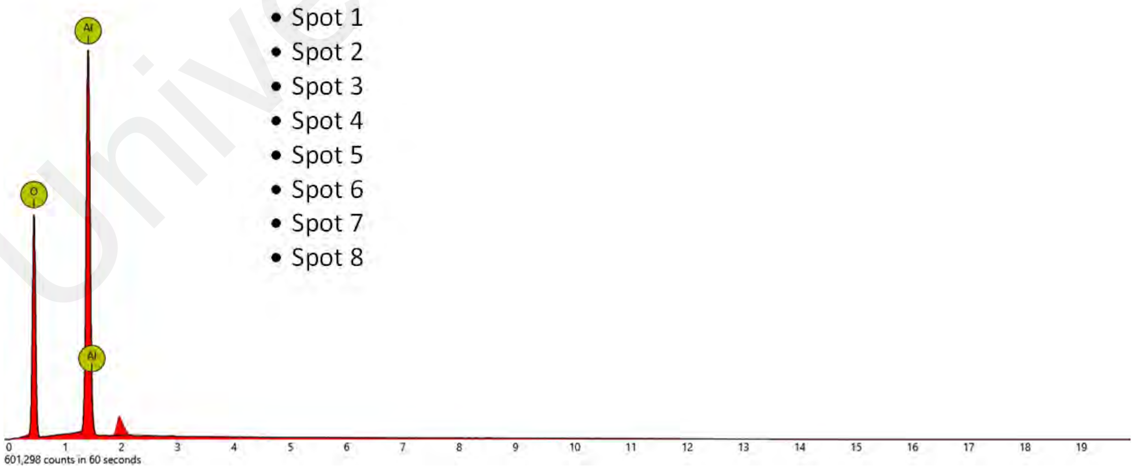

Figure 4.3: EDS spectra of the eight spots shown in Figure 4.2.

Table 4.1: Elemental percentages obtained from EDS analysis.

Element	Atomic (%)	Weight (%)
O	66.42	53.97
Al	33.58	46.03
Total	100 %	100 %

4.1.2 Densification

Figure 4.4 presents a relative density as a function of sintering temperature and manganese content graph. Samples were sintered in conventional furnace for 2 hours. At low sintering temperature (1300 °C), undoped alumina densified better than manganese-doped alumina with 0.1-Mn samples achieving significantly lower densities than other tested samples. Figure 4.5e evidences the slow densification rate of 0.1-Mn sample at 1300 °C. Figure 4.5e indicates that densification process was still at an early stage where only necking between the particles can be seen without grain boundaries. 1.0-Mn samples showed the fastest sintering rate among all doped samples at this low sintering temperature (Figure 4.5m).

At 1400 °C, the densification rate of manganese-doped samples increased to match and surpass the density of undoped samples. At this temperature samples containing high manganese content (0.5 and 1.0 wt. %) showed enhanced densification relative to undoped alumina.1.0-Mn samples developed distinct and clear grain boundaries (Figure 4.5n) in comparison to other tested samples. 0.1-Mn continued to show slow sintering rate at 1400 °C.

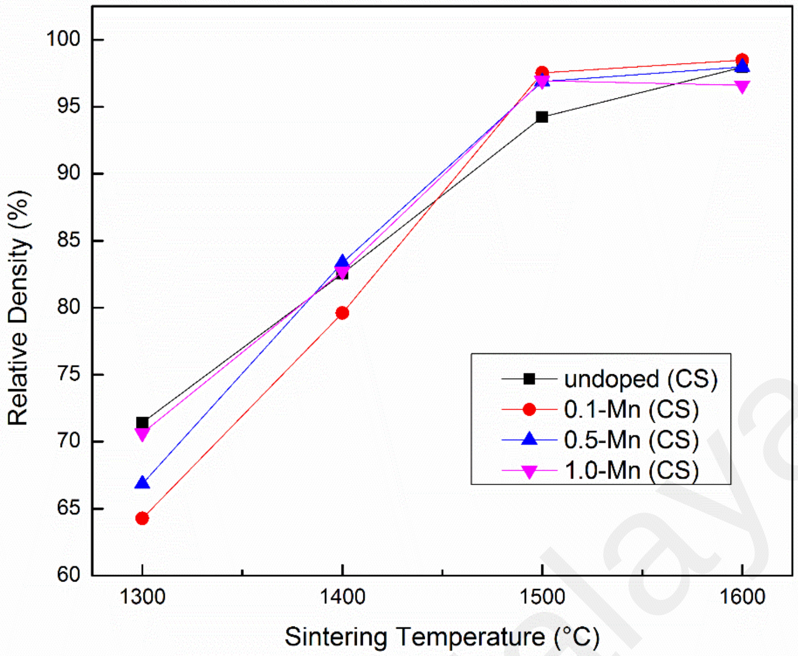

Figure 4.4: Variation of density with sintering temperature of undoped and doped samples sintered using conventional sintering.

An interesting sintering behaviour happened at 1500 °C, all manganese-doped samples achieved significantly higher relative densities than undoped samples and 0.1-Mn samples showed significant increase in the sintering rate at this temperature. Manganese-doped samples could sinter to relative densities of ≈ 97 %, while undoped samples could only achieve relative densities of 94 %. 0.1-Mn could sinter to 97.5 % relative density. The microstructure of manganese-doped alumina sintered at 1500 °C (Figure 4.5g, k, and o) show completed densification with some intergranular and intergranular closed pores, while undoped alumina microstructure (Figure 4.5c) contains open pores which evidences incomplete densification.

At 1600 °C, the densification rate of manganese-doped samples dropped significantly resulting in small increment in the densities of 0.1-Mn and 0.5-Mn samples. In contrast to doped samples, undoped samples continued to densify at a densification rate similar to the densification rate at lower sintering temperatures. At this sintering temperature, the final densities of all samples did not vary significantly. 0.1-Mn samples achieved the highest relative densities (98.5 %) of all tested powder compositions. Undoped samples developed inhomogeneous microstructure (Figure 4.5d), whereas manganese-doped samples developed more homogeneous microstructures (Figure 4.5h, i, and p) at this high sintering temperature.

Interestingly, one may observe a small density drop for 1.0-Mn samples sintered at 1500 °C. Previous published studies reported a similar behavior in other manganese-doped ceramic materials when sintering at high temperatures for prolonged times. This phenomenon is typically known as desintering or dedensification. Desintering is the reduction of the density of a sample during sintering. Desintering was attributed manganese evaporation at high temperatures (Chang et al., 2013; Li et al., 2017; Wu et al., 2017). Moreover, Abnormal grain growth is also believed to cause desintering in ceramics where large grains hinders the growth of finer grains by exerting tensile stresses on them (Demartin et al., 1997).

The insignificant variation in the densification of manganese-doped samples and undoped sample sintered at temperatures exceeding 1500 °C is in good agreement with previous studies (Erkalfa et al., 1995; Sathiyakumar & Gnanam, 2002). Erkalfa et al. (1995) obtained densities in the range of 98 – 99 % for both undoped and manganese-doped samples at 1600 °C.

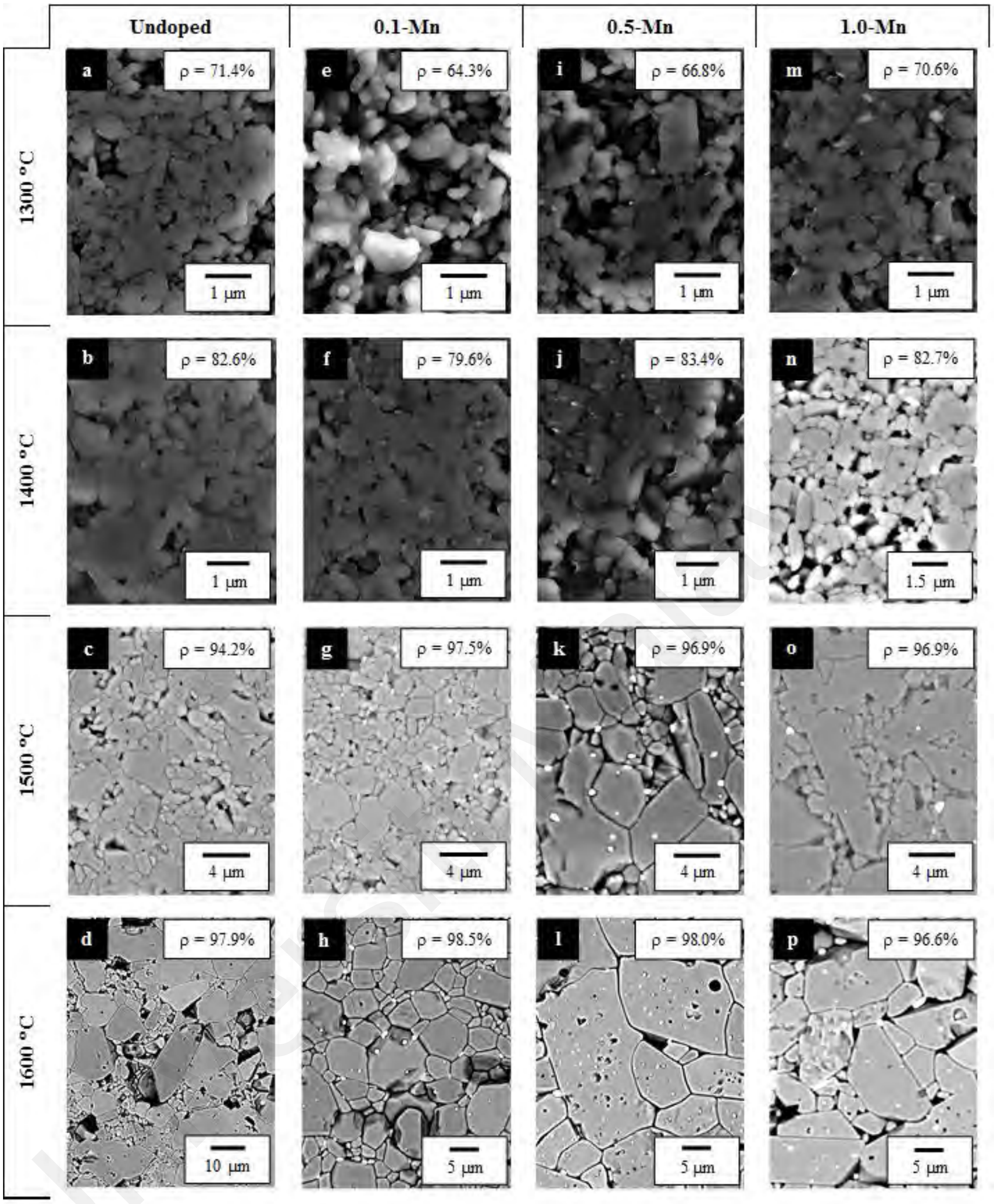

Figure 4.5: SEM micrographs of undoped and manganese-doped samples sintered in conventional furnace at 1300, 1400, 1500 and 1600 °C.

Sathiyakumar and Gnanam (2002) also obtained 98 % relative density for undoped samples and relative density in the range of 98 – 99 % for manganese-doped samples. Therefore, this variation in density between undoped and manganese-doped samples is insignificant and is in good agreement with our current results.

Furthermore, the observed effectiveness of 0.1 wt. % manganese addition on the densification of alumina is consistence with what was previous literature (Keski & Cutler, 1968; Keski & Cutler, 1965). According to Keski and Cutler the densification rate of alumina was enhanced by manganese addition up to 0.3 wt. %, thereafter the densification rate dropped.

4.1.3 Grain Growth

0.1 wt. % manganese addition did not only resulted in enhanced densification but also in grain growth hindrance. Figure 4.6 shows average grain size versus density trajectory as a function of dopant concentration. 0.1-Mn samples yielded the lowest average grain size of all tested samples even though it had the highest relative density. From Figure 4.6, we can observe that the grain growth process was insignificant at relative density below 90 % and low sintering temperatures (1300 and 1400 °C). In this relative density range and at these low sintering temperatures, and all samples had comparable grain size.

Grain growth was evident when the samples' densities exceeds 95 % (Figure 4.6) and when the sintering temperature increased to 1500 and 1600 °C (Figure 4.7). In this high grain growth region, 1.04 µm average grain size was obtained for 0.1-Mn samples at sintering temperature of 1500 °C and 97.5 % relative density, while undoped samples yielded higher average grain size (1.23 µm) at a relative density value of only 94 %. Both 0.1-Mn samples and undoped samples developed homogeneous microstructures at 1500 °C (Figure 4.5g and c). Moreover, this low average grain size of 0.1-Mn specimens is in close approximation to what was previously reported (Zuo et al., 2015) for the renowned grain growth supressing additive, MgO. At 1500 °C, 0.5-Mn and 1.0-Mn samples showed moderate grain growth (average grain size of 1.96 µm and 2.37 µm, respectively) which is accompanied by inhomogeneous microstructure. Small grains were trapped between larger grains (Figure 4.5k and o). In addition, 1.0-Mn alumina developed platelet grains as large as 20 µm with aspect ratio of 5.

Abnormal grain growth was evident for 0.5-Mn and 1.0-Mn samples sintered at 1600 °C (Figure 4.5i and p). At 1600 °C, grain growth dominated over densification particularly in high manganese content samples resulting in abnormal grain growth with grains as large as 50 µm. These samples experienced small density increment with abnormal grain growth. 0.1-Mn maintained their homogeneous microstructure and yielded the smallest average grain size at this elevated sintering temperature. Interestingly, undoped samples developed inhomogeneous microstructure (Figure 4.5d). this contradicted previous studies (Erkalfa et al., 1995; Sathiyakumar & Gnanam, 2002) which reported inhomogeneous microstructure in manganese-doped samples in comparison to undoped samples.

To summarise, 0.1 wt. % manganese addition resulted in significant densification enhancement, grain growth hindrance, and microstructure homogenization in alumina particularly at 1500 °C. Higher manganese contents (0.5 wt. % and 1.0 wt. %) resulted in abnormal grain growth.

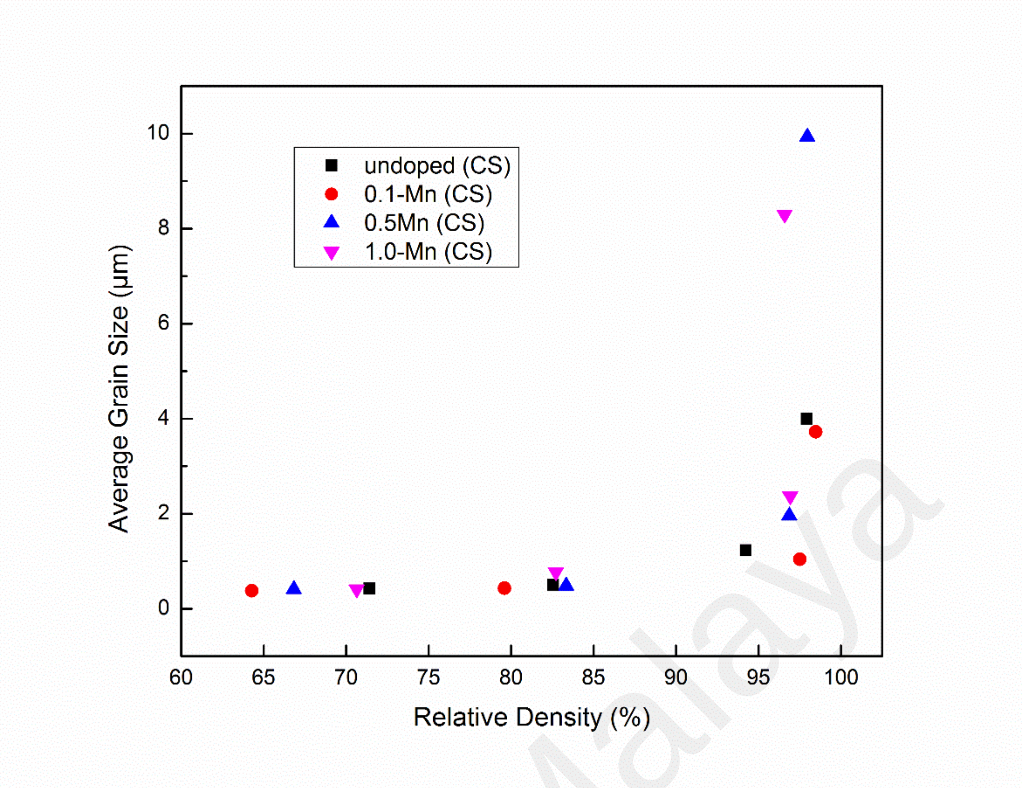

Figure 4.6: Average grain size vs relative density trajectory of undoped and manganese-doped alumina.

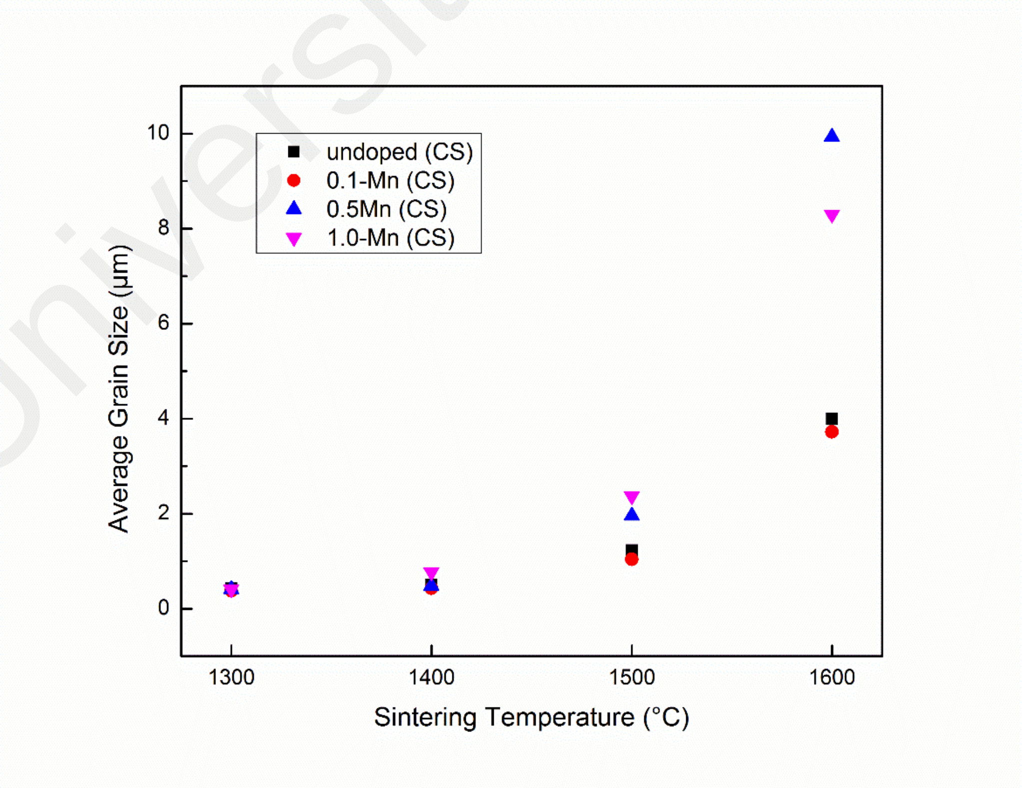

Figure 4.7: Effect of sintering temperature on the grain growth process.

A possible explanation to the role of manganese in the observed densification enhancement is that densification can be expressed as the movement of atoms between grains across grain boundaries. Manganese change its valence state (reduction from Mn^{4+} to Mn^{2+}) upon heating. As a result to this change in the valence state, and the charge unbalance, vacancies or interstitials can be created to maintain electrical neutrality which increase the grain boundary mobility and atomic movements (Erkalfa et al., 1995; Li et al., 2017; Roy & Coble, 1968).

4.1.4 Hardness

Figure 4.8 Shows hardness as a function of sintering temperature and dopant concentration. Undoped specimens showed almost a linear increase of hardness with sintering temperature, whereas manganese-doped specimens showed different trends. 1.0-Mn alumina had higher hardness relative to other samples at low sintering temperatures (1300 and 1400 °C), but the hardness value started to drop as the sintering temperature increased to 1500 and 1600 °C. At sintering temperature of 1400 °C, although both undoped samples and 1.0-Mn samples had relative density of ≈ 83%, there is a palpable difference in the hardness between the two samples. This suggests that the presence of manganese plays a positive role in improving hardness of alumina. At 1500 °C, all manganese-doped samples had significantly higher hardness than undoped alumina. In particular, 0.1-Mn alumina had the highest hardness value (≈15 GPa), which associated with the improved densification of manganese-doped samples.

As the sintering temperature increased to 1600 °C, however, all manganese-doped samples showed hardness decrement presumably due to the increased grain growth at high sintering temperature. At 1500 and 1600 °C, there are samples with very similar relative densities (Figure 4.4), yet different hardness values can be observed (Figure 4.8). This variation in hardness values can be explained by the differences in average grain size between these samples. Mechanical properties and hardness are directly associated with grain size based on the empirical Hall-Petch relationship from which a material hardness increases with decreasing grain size (Wollmershauser et al., 2014).

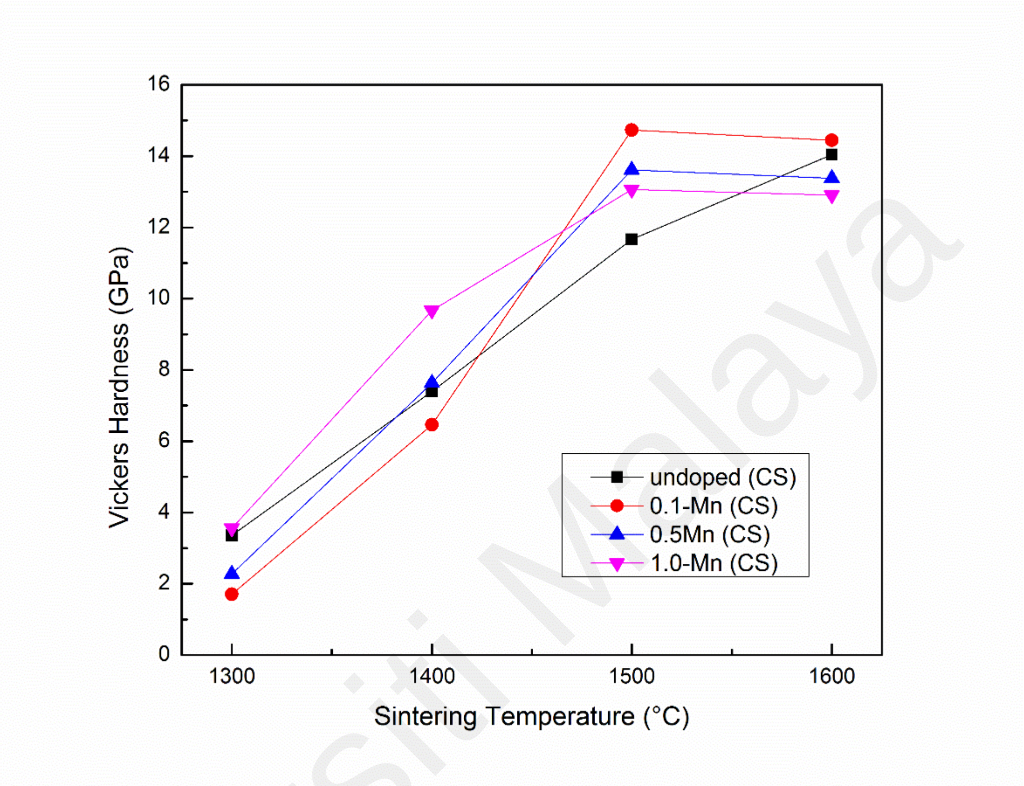

Figure 4.8: Effect of sintering temperature and manganese content on the hardness of conventionally-sintered alumina.

The hardness values we report in this study are different from those reported by Erkalfa et al. (1995) and Sathiyakumar & Gnanam (2002). This variation in hardness values can be explained by the light indentation loads that were used in these two previous studies. Indentation loads of 0.5 KgF and 2.0 KgF were applied by (Erkalfa et al. (1995) and Sathiyakumar & Gnanam (2002), respectively. According to Krell (1998), indentation load and grain size have a significant effect on the hardness value accuracy of ceramic materials. For 3 μm grain size, hardness value can increase from 18 GPa to 23 GPa when the indention load is decreased from 10 KgF to 0.4 KgF.

4.2 Conventional Sintering and Microwave Sintering Comparison

4.2.1 Phase Evolution

Figure 4.9 presents XRD patterns of samples sintered in microwave furnace and conventional furnace at 1500 °C. The XRD patterns evidences that the second phase spinel ($MnAl_2O_4$) intensity is similar in microwave-sintered and conventionally-sintered samples. Phase evolution of manganese-doped alumina was similar in microwave sintering and conventional sintering. For more discussions on the phase evolution of manganese-doped alumina, please refer to section 4.1.1.

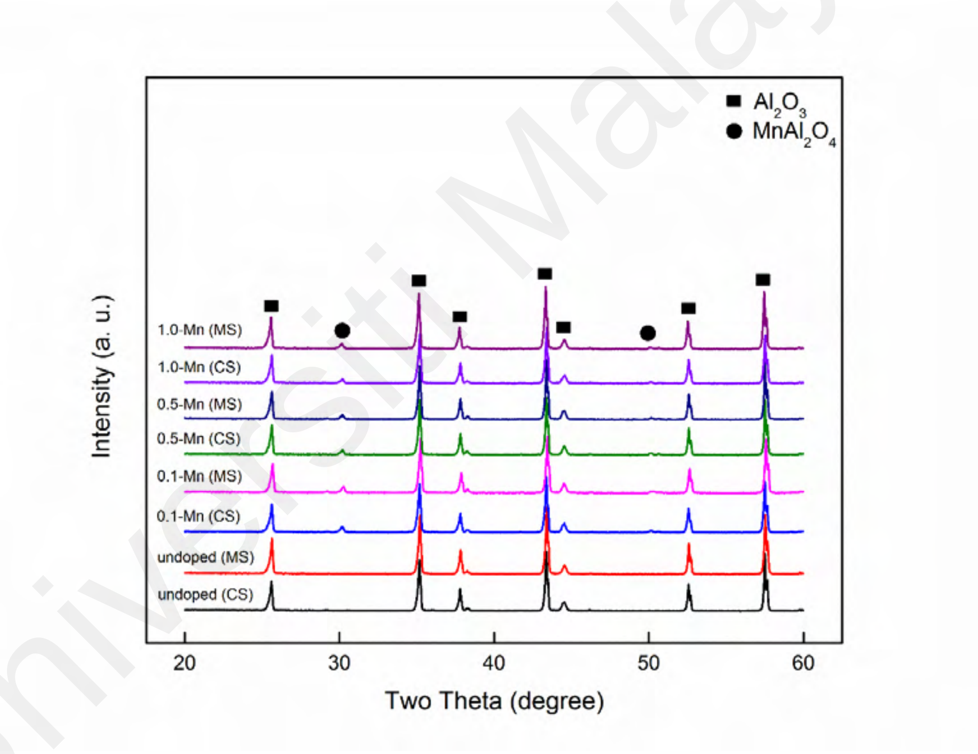

Figure 4.9: XRD patterns of microwave-sintered and conventionally-sintered samples.

4.2.2 Densification

In terms of densification, microwave-sintered alumina followed similar trend as conventionally-sintered alumina. At sintering temperature of 1300 °C, undoped samples densified better than manganese-doped samples. As the sintering temperature increased to 1400 °C, the densification kinetics of manganese-doped alumina increased and 1.0-Mn alumina surpassed the density of undoped alumina. At 1500 °C, all manganese-doped samples showed significantly higher relative densities than that of undoped alumina. All manganese-doped samples achieved relative densities of ≈ 92 %, while undoped samples achieved relative densities of 88 % (Figure 4.10). Figure 4.10 shows variation of final relative density with sintering temperature and manganese content of microwave sintered alumina.

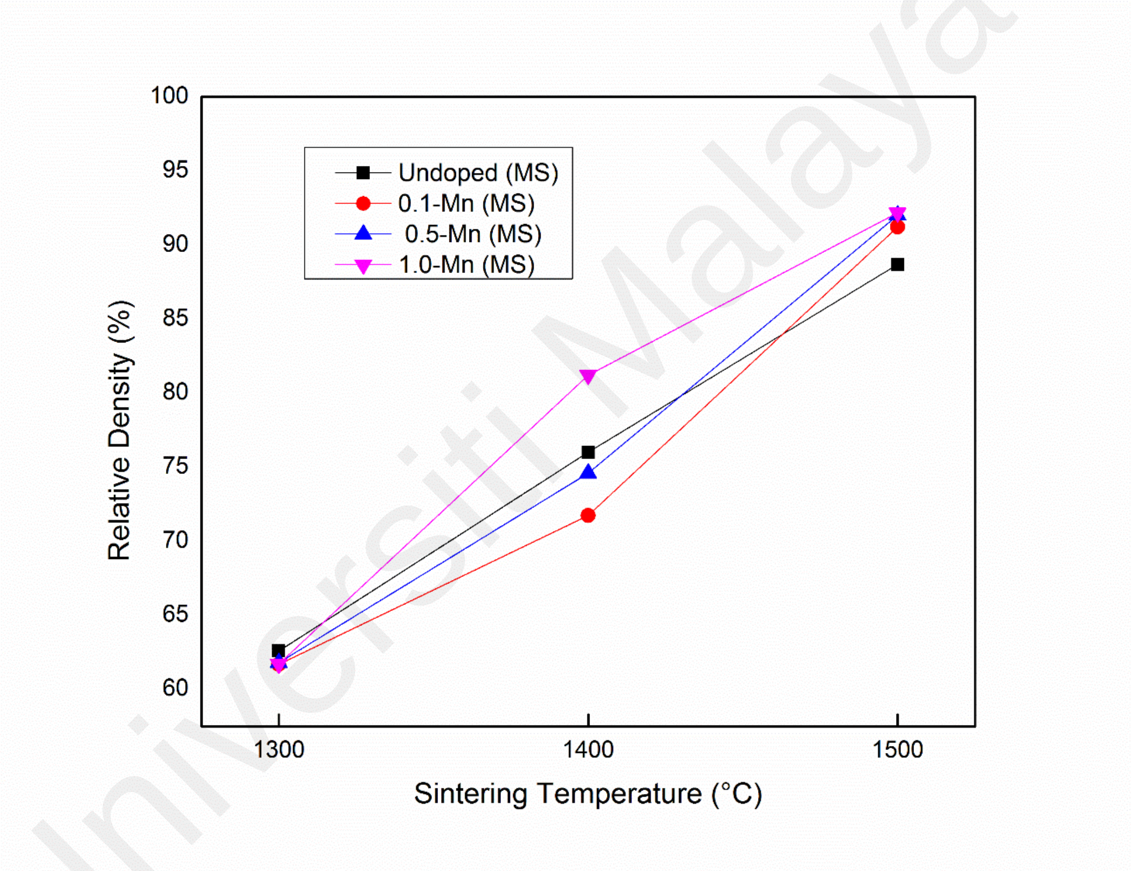

Figure 4.10: Variation of final relative density with sintering temperature and manganese content of microwave sintered alumina.

All microwave-sintered samples achieved lower relative densities than their conventionally-sintered counterparts. Figure 4.11 and Table 4.2 show comparison between the final relative densities of conventionally and microwave sintered samples.

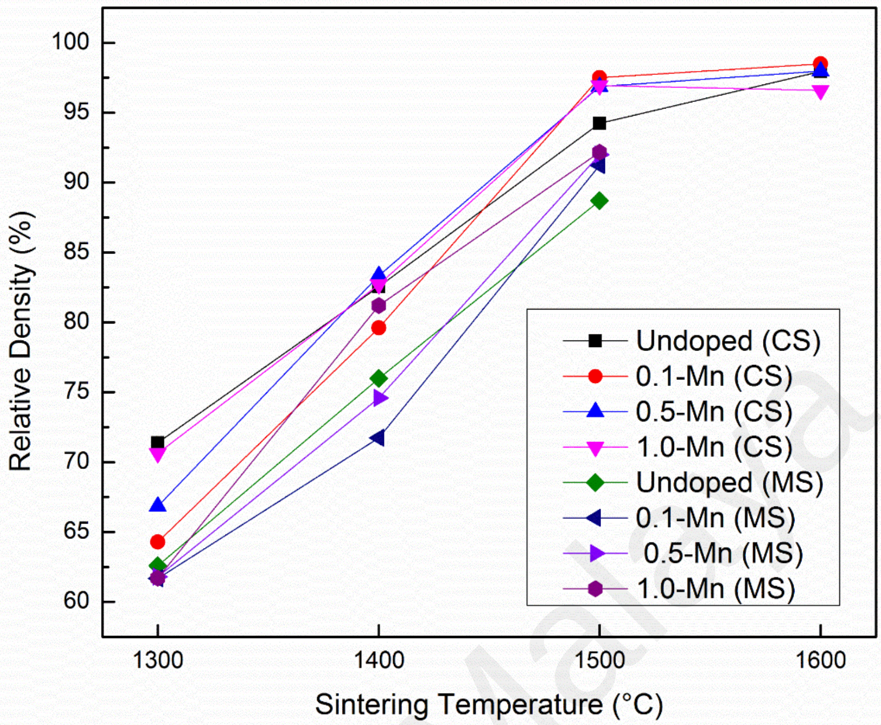

Figure 4.11: Comparison of final densities obtained using conventional sintering and microwave sintering for different sample compositions.

The variation in relative densities between conventionally-sintered and microwave-sintered alumina can be explained by the short dwell time (5 minutes) that was applied in microwave sintering in comparison to 2-hour dwell time for conventional sintering. The difference in density between microwave-sintered samples and conventionally-sintered samples is ≈ 5 % at 1500 °C. This percentage difference is similar to what was reported in the literature. According to Croquesel et al. (2016), at sintering temperature of 1550 °C, powders having 250 nm particle size reached lower relative densities when sintered using microwaves relative to conventional sintering. Densities reported by Croquesel et al. (2016) were 89.5% for conventionally-sintered alumina, and 84.8% for microwave sintered alumina. It is noteworthy that Croquesel et al. used a novel single mode microwave furnace which enabled more accurate temperature measurements.

Table 4.2: Microwave sintering and conventional sintering final relative density comparison.

Powder	Sintering temperature (°C)	Final relative density (CS) (%)	Final relative density (MS) (%)
undoped	1300	71.4	62.6
	1400	82.5	76.1
	1500	94.2	88.7
	1600	97.9	-
0.1-Mn	1300	64.3	61.7
	1400	79.6	71.7
	1500	97.5	91.2
	1600	98.5	-
0.5-Mn	1300	66.8	61.8
	1400	83.5	74.6
	1500	96.9	92.0
	1600	98	-
1.0-Mn	1300	70.6	61.7
	1400	82.7	81.2
	1500	96.9	92.2
	1600	96.6	-

4.2.3 Grain Growth

As far as grain growth is concerned, microwave-sintered alumina exhibited similar grain growth trend to what was observed in conventionally-sintered alumina (Figure 4.6). Figure 4.12 show average grain size versus density trajectory of microwave-sintered samples. 0.1-Mn specimens developed the lowest average grain growth of all tested specimens and 1.0-Mn samples developed the largest average grain size.

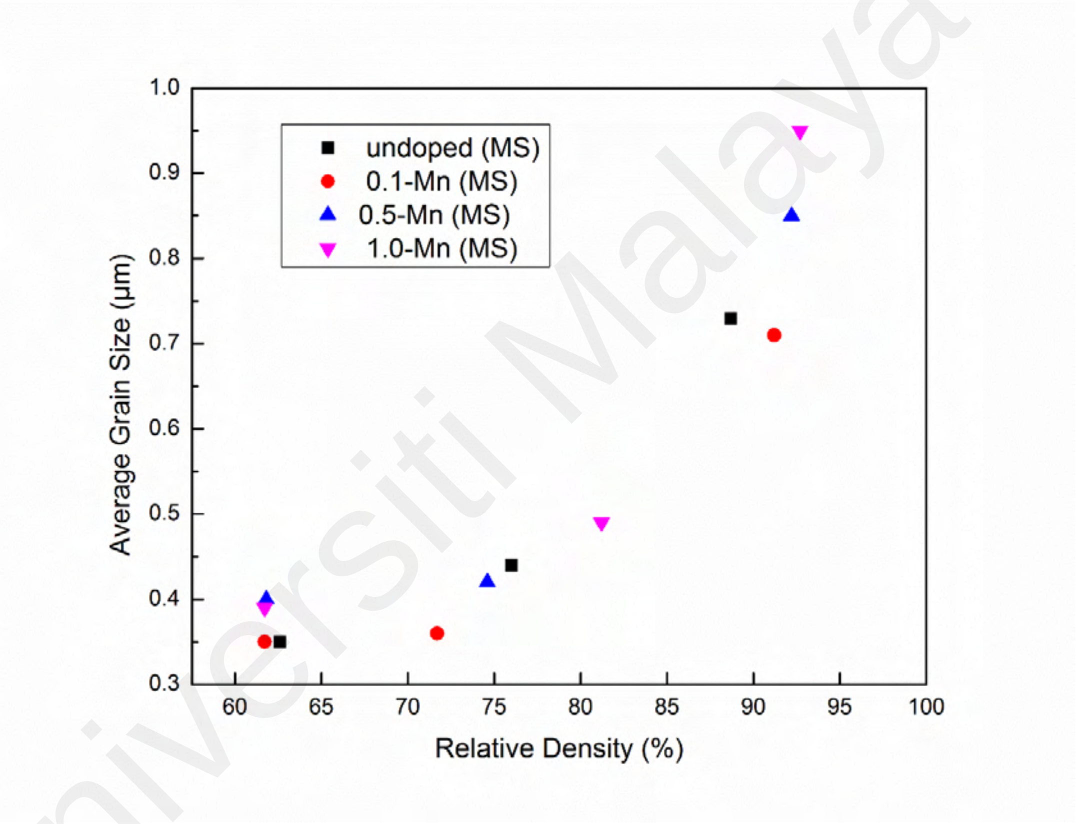

Figure 4.12: Average grain size vs density trajectory of microwave-sintered samples.

In general, the relative density of microwave-sintered samples were lower than the conventionally-sintered samples. However, microwave sintering was beneficial in retarding the grain coarsening of alumina i.e. all the samples had grain sizes of below 1 μm. The comparison of the microstructure evolution of the microwave-sintered and conventionally-sintered samples is shown in Figure 4.13.

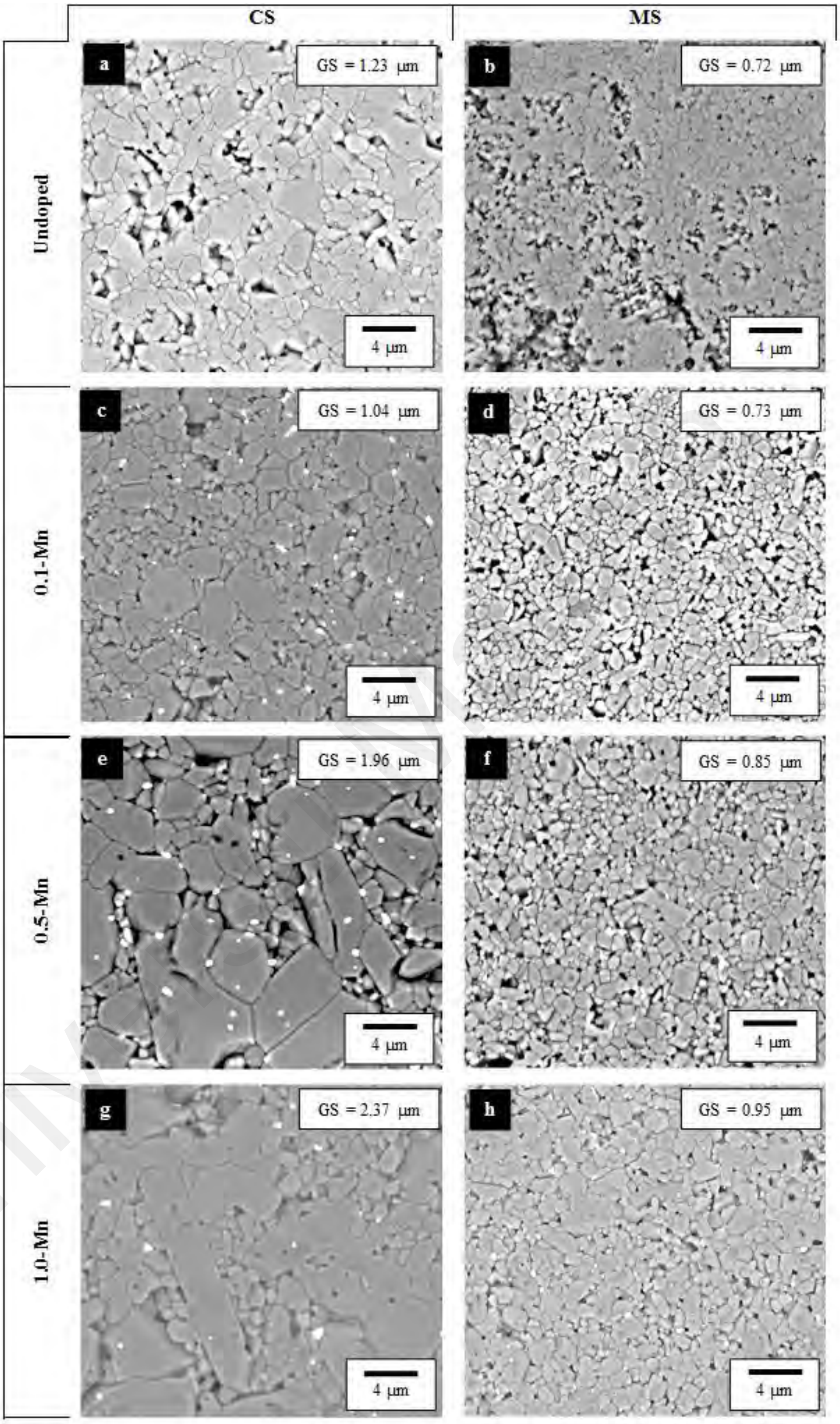

Figure 4.13: SEM micrographs comparing the microstructure evolution (1500 °C) between the conventional sintered (CS) and microwave sintered (MS) alumina. The average grain size (GS) of the sample is as shown in the micrograph.

The observed grain growth retardation in microwave sintered samples correlates well with the literature (Golestani et al., 2011; Demirskyi et al., 2013; Ramesh et al., 2018). Grain growth retardation in microwave sintering might be caused by the high heating rates applied in microwave sintering (Menezes & kiminami, 2008). From Figure 4.13, it is clear that conventionally-sintered samples and manganese-doped samples in particular possess microstructure with a few isolated pores, whereas microwave sintered samples possess microstructure with open pores which indicates incomplete densification. At density of ≈ 92 %, microwave-sintered samples were still at end of the intermediate stage of sintering (German, 2014), and conventionally-sintered samples were well within the final stage of sintering.

4.2.4 Hardness

Vickers Hardness of microwave-sintered and conventionally-sintered alumina are contrasted in Figure 4.14. Microwave-sintered alumina exhibited lower hardness values than that of conventionally-sintered alumina. The lower hardness values corresponds to lower densities achieved by microwave-sintered samples. An interesting trend can be observed for 1.0-Mn samples, At sintering temperature of 1500 °C, there is a small difference in hardness values between conventionally-sintered and microwave-sintered samples (13 and 12.2 GPa, respectively) even though there is a significant difference in relative densities (97 % and 92.7 %, respectively). This is due to the drop in the hardness of 1.0-Mn during the final stage of sintering and the relative increase in hardness during the intermediate stage of the sintering process (see Figure 4.8). This drop in hardness is presumably due to the exaggerated grain growth during the final stage of sintering.

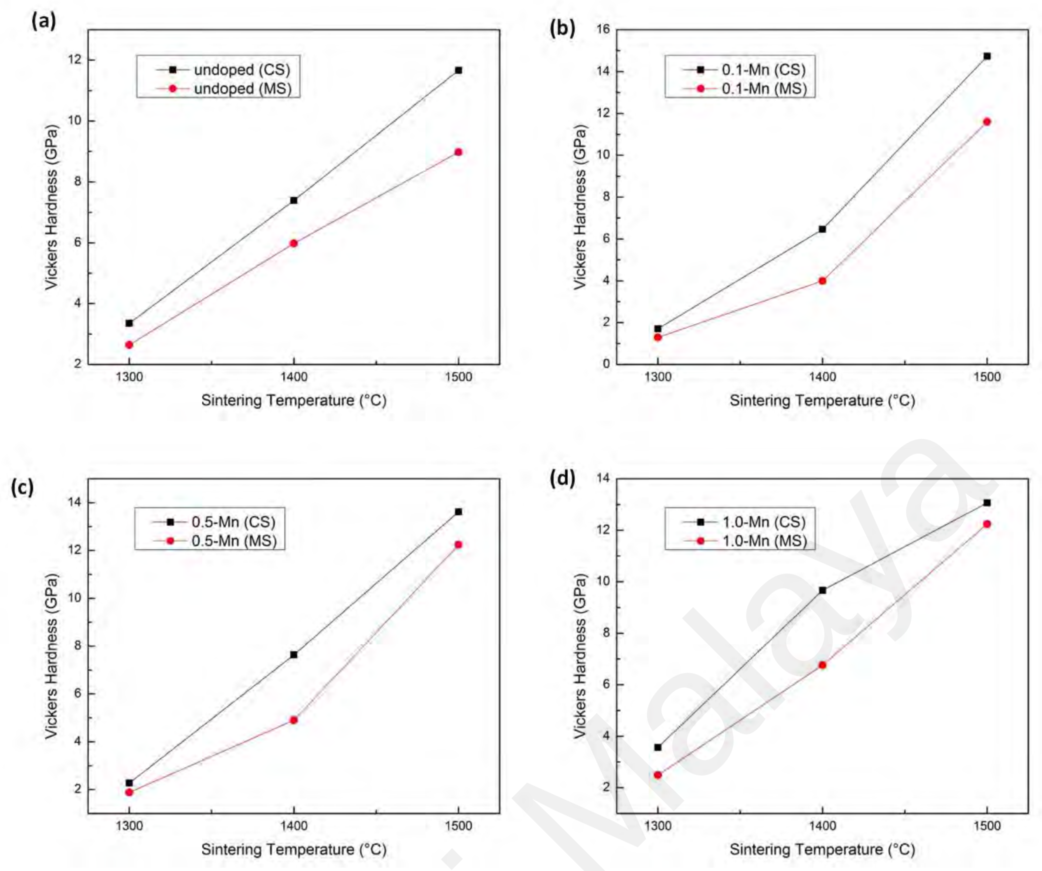

Figure 4.14: Vickers hardness as a function of manganese content and sintering temperature.

CHAPTER 5: CONCLUSIONS AND FURTHER WORK

5.1 Conclusions

The densification, microstructural evolution, phase analysis, and hardness of alumina containing manganese oxide in different concentration levels (0.1, 0.5, and 1.0 wt. %) were studied. The alumina and manganese mixture was prepared using wet milling process. Ceramic compacts were sintered in conventional furnace at 1300, 1400, 1500, and 1600 °C with 2-hour holding time. Microwave sintering was carried out in multimode microwave furnace at 1300, 1400, and 1500 °C with 5-minute holding time. The main conclusions that can be drawn from this study are:

1. XRD analysis revealed the development of spinel second phase ($MnAl_2O_4$) in manganese-doped alumina which indicates a limited or no solubility of manganese in alumina.
2. 0.1 wt. % manganese concentration significantly enhanced the densification process of alumina at 1500 °C sintering temperature. At 1500 °C, samples with 0.1 wt. % manganese content could sinter to 97.5 % relative density in comparison to 94.2 % relative density for undoped alumina.
3. 0.1 wt. % manganese concentration hindered grain growth of alumina resulting in the lowest average grain size of all tested compositions at all sintering temperatures.
4. 0.1 wt. % manganese concentration produced homogeneous microstructure, particularly at high sintering temperatures (1500 and 1600 °C) and high density (>95 %) where grain growth is most severe.
5. Higher manganese concentrations (0.5 and 1.0 wt. %) resulted in inhomogeneous grain growth at 1500 °C and abnormal grain growth at 1600 °C.

6. Microwave sintering was not beneficial in improving the densification of neither undoped nor doped samples. However, microwave sintering was beneficial in grain coarsening retardation.
7. Based on Vickers Hardness test, at 1500 °C, samples with 0.1 wt. % exhibited significantly higher hardness than undoped samples which is associated with greater relative density value and smaller grain size.

5.2 Further Work

Based on the results of this study, future work suggestions are:

1. Perform Transmission electron microscopy (TEM) studies on the manganese doped alumina especially 1.0-Mn samples. This may provide some insight into the segregation of manganese at the grain boundary region.
2. It has been shown that 0.1 wt. % manganese concentration significantly enhanced the densification and hindered grain growth of alumina sintered at 1500 °C, it would be interesting to see how this particular manganese concentration behaves in two-step sintering.

REFERENCES

Acchar, W., & Ramalho, E. G. (2008). Effect of MnO2 addition on sintering behavior of tricalcium phosphate: Preliminary results. *Materials Science and Engineering: C, 28*(2), 248-252.

Agrawal, D. (2006). *Microwave sintering, brazing and melting of metallic materials.* Paper presented at the Sohn International Symposium; Advanced Processing of Metals and Materials Volume 4: New, Improved and Existing Technologies: Non-Ferrous Materials Extraction and Processing.

Alford, N. M., & Penn, S. J. (1996). Sintered alumina with low dielectric loss. *Journal of Applied Physics, 80*(10), 5895-5898.

Bae, I. J., & Baik, S. (1997). Abnormal grain growth of alumina. *Journal of the American Ceramic Society, 80*(5), 1149-1156.

Bae, S. I., & Baik, S. (1993). Determination of critical concentrations of silica and/or calcia for abnormal grain growth in alumina. *Journal of the American Ceramic Society, 76*(4), 1065-1067.

Bagley, R. D., Cutler, I. B., & Johnson, D. L. (1970). Effect of TiO2 on initial sintering of Al2O3. *Journal of the American Ceramic Society, 53*(3), 136-141.

Baik, S., & Moon, J. H. (1991). Effects of magnesium oxide on grain-boundary segregation of calcium during sintering of alumina. *Journal of the American Ceramic Society, 74*(4), 819-822.

Bennison, S. J., & Harmer, M. P. (1983). Effect of MgO solute on the kinetics of grain growth in A12O3. *Journal of the American Ceramic Society, 66*(5).

Bernardgranger, G., & Guizard, C. (2007). Influence of MgO or TiO2 doping on the sintering path and on the optical properties of a submicronic alumina material. *Scripta Materialia, 56*(11), 983-986.

Berry, K. A., & Harmer, M. P. (1986). Effect of MgO solute on microstructure development in Al2O3. *Journal of the American Ceramic Society, 69*(2), 143-149.

Bhattacharya, M., & Basak, T. (2016). A review on the susceptor assisted microwave processing of materials. *Energy, 97*, 306-338.

Binner, J., Vaidhyanathan, B., Wang, J., Price, D., & Reading, M. (2007). Evidence for non-thermal microwave effects using single and multimode hybrid conventional/microwave systems. *Journal of Microwave Power and Electromagnetic Energy, 42*(2), 47-63.

Bodišová, K., Galusek, D., Švančárek, P., Pouchlý, V., & Maca, K. (2015). Grain growth suppression in alumina via doping and two-step sintering. *Ceramics International, 41*(9), 11975-11983.

Brosnan, K. H., Messing, G. L., & Agrawal, D. K. (2003). Microwave sintering of alumina at 2.45 GHz. *J. Am. Cer. Soc, 86*(8), 1307-1312.

Bykov, Y. V., Egorov, S., Eremeev, A., Kholoptsev, V., Plotnikov, I., Rybakov, K., . . . Sorokin, A. (2010). Effects of microwave heating in nanostructured ceramic materials. *Powder Metallurgy and Metal Ceramics, 49*(1-2), 31-41.

Carter, C. B., & Norton, M. G. (2007). *Ceramic materials: science and engineering*: Springer Science & Business Media.

Castro, R., & van Benthem, K. (2012). *Sintering: mechanisms of convention nanodensification and field assisted processes* (Vol. 35): Springer Science & Business Media.

Castro, R. H., & Gouvêa, D. (2016). Sintering and nanostability: the thermodynamic perspective. *Journal of the American Ceramic Society, 99*(4), 1105-1121.

Chan, T.-Y., Liu, S.-J., & Lin, S.-T. (1998). Effects of high concentrations of liquid phase and magnesia on the grain growth of alumina. *Ceramics International, 24*(8), 617-625.

Chang, C.-H., Rufner, J. F., Benthem, K. v., & Castro, R. H. (2013). Design of desintering in tin dioxide nanoparticles. *Chemistry of Materials, 25*(21), 4262-4268.

Chen, P. L., & Chen, I. W. (1996). Grain growth in CeO2: dopant effects, defect mechanism, and solute drag. *Journal of the American Ceramic Society, 79*(7), 1793-1800.

Cheng, J., Agrawal, D., Zhang, Y., & Roy, R. (2002). Microwave sintering of transparent alumina. *Materials Letters, 56*(4), 587-592.

Cho, J., Harmer, M. P., Chan, H. M., Rickman, J. M., & Thompson, A. M. (1997). Effect of yttrium and lanthanum on the tensile creep behavior of aluminum oxide. *Journal of the American Ceramic Society, 80*(4), 1013-1017.

Chong, F. D., Tan, C. Y., Singh, R., Muchtar, A., Somalu, M. R., Ng, C. K., . . . Tan, Y. M. (2016). Effect of manganese oxide on the sinterability of 8 mol% yttria-stabilized zirconia. *Materials Characterization, 120*, 331-336.

Clark, D. E., & Sutton, W. H. (1996). Microwave processing of materials. *Annual Review of Materials Science, 26*(1), 299-331.

Clavel, G., Willinger, M. G., Zitoun, D., & Pinna, N. (2008). Manganese-Doped Zirconia Nanocrystals. *European Journal of Inorganic Chemistry, 2008*(6), 863-868.

Coble, R. L. (1961). Sintering Crystalline Solids. II. Experimental Test of Diffusion Models in Powder Compacts. *Journal of Applied Physics, 32*(5), 793-799.

Coble, R. L. (1962). Transparent alumina and method of preparation: Google Patents.

Croquesel, J., Bouvard, D., Chaix, J.-M., Carry, C. P., Saunier, S., & Marinel, S. (2016). Direct microwave sintering of pure alumina in a single mode cavity: Grain size and phase transformation effects. *Acta Materialia, 116*, 53-62.

Croquesel, J., Carry, C. P., Chaix, J.-M., Bouvard, D., & Saunier, S. (2017). Direct Microwave Sintering of Alumina in a Single Mode Cavity: Magnesium doping effects. *Journal of the European Ceramic Society*.

Delaunay, D., Huntz, A., & Lacombe, P. (1980). The Influence of yttrium on the sintering of Al2O3. *Journal of the Less Common Metals, 70*(1), 115-117.

Demartin, M., Hérard, C., Carry, C., & Lemaître, J. (1997). Dedensification and anomalous grain growth during sintering of undoped barium titanate. *Journal of the American Ceramic Society, 80*(5), 1079-1084.

Demirskyi, D., Agrawal, D., & Ragulya, A. (2013). Comparisons of grain size-density trajectory during microwave and conventional sintering of titanium nitride. *Journal of Alloys and Compounds, 581*, 498-501.

Dey, S., Chang, C.-H., Gong, M., Liu, F., & Castro, R. H. (2015). Grain growth resistant nanocrystalline zirconia by targeting zero grain boundary energies. *Journal of Materials Research, 30*(20), 2991-3002.

Dey, S., Mardinly, J., Wang, Y., Valdez, J. A., Holesinger, T. G., Uberuaga, B. P., . . . Castro, R. H. (2016). Irradiation-induced grain growth and defect evolution in nanocrystalline zirconia with doped grain boundaries. *Phys Chem Chem Phys, 18*(25), 16921-16929.

Dillon, S. J., & Harmer, M. P. (2008). Demystifying the role of sintering additives with “complexion”. *Journal of the European Ceramic Society, 28*(7), 1485-1493. doi:10.1016/j.jeurceramsoc.2007.12.018

Dillon, S. J., Harmer, M. P., & Rohrer, G. S. (2010). Influence of interface energies on solute partitioning mechanisms in doped aluminas. *Acta Materialia, 58*(15), 5097-5108.

Ehre, D., & Chaim, R. (2008). Abnormal Hall–Petch behavior in nanocrystalline MgO ceramic. *Journal of Materials Science, 43*(18), 6139-6143.

Erkalfa, H., Misirli, Z., & Baykara, T. (1995). Densification of Alumina at 1250°C with MnO2 and TiO2 additives.pdf. *Ceramics International, 21*, 345-348.

Erkalfa, H., Misirli, Z., Demirci, M., Toy, C., & Baykara, T. (1995). The densification and microstructural development of Al2O3 with manganese oxide addition. *Journal of the European Ceramic Society, 15*(2), 165-171.

Fang, J., Thompson, A. M., Harmer, M. P., & Chan, H. M. (1997). Effect of Yttrium and Lanthanum on the Final-Stage Sintering Behavior of Ultrahigh-Purity Alumina. *Journal of the American Ceramic Society, 80*(8), 2005-2012.

Fang, Y., Cheng, J., & Agrawal, D. K. (2004). Effect of powder reactivity on microwave sintering of alumina. *Materials Letters, 58*(3-4), 498-501.

Galusek, D., Ghillányová, K., Sedláček, J., Kozánková, J., & Šajgalík, P. (2012). The influence of additives on microstrucutre of sub-micron alumina ceramics prepared by two-stage sintering. *Journal of the European Ceramic Society, 32*(9), 1965-1970.

Galusek, D., Sedláček, J., Chovanec, J., & Michálková, M. (2015). The influence of MgO, Y2O3 and ZrO2 additions on densification and grain growth of submicrometre alumina sintered by SPS and HIP. *Ceramics International, 41*(8), 9692-9700.

Gavrilov, K. L., Bennison, S. J., Mikeska, K. R., Chabala, J. M., & Levi-Setti, R. (1999). Silica and Magnesia Dopant Distributions in Alumina by High-Resolution Scanning Secondary Ion Mass Spectrometry. *Journal of the American Ceramic Society, 82*(4), 1001-1008.

German, R. (2014). *Sintering: from empirical observations to scientific principles*: Butterworth-Heinemann.

Golestani-fard, F., Mazaheri, M., Aminzare, M., & Ebadzadeh, T. (2011). Microstructural evolution of a commercial ultrafine alumina powder densified by different methods. *Journal of the European Ceramic Society, 31*(14), 2593-2599.

Greskovich, C., & Brewer, J. A. (2001). Solubility of magnesia in polycrystalline alumina at high temperatures. *Journal of the American Ceramic Society, 84*(2), 420-425.

Gunnewiek, R. F. K., & Kiminami, R. H. G. A. (2014). Effect of heating rate on microwave sintering of nanocrystalline zinc oxide. *Ceramics International, 40*(7), 10667-10675.

Hall, E. (1951). Proc. Phys. Soc. *Series B, 64*, 747.

Handwerker, C. A., Morris, P. A., & Coble, R. L. (1989). Effects of chemical inhomogeneities on grain growth and microstructure in Al2O3. *Journal of the American Ceramic Society, 72*(1), 130-136.

Horn, D. S., & Messing, G. L. (1995). Anisotropic grain growth in TiO2-doped alumina. *Materials Science and Engineering: A, 195*, 169-178.

Huesup, S., & L., C. R. (1990). Origin and Growth Kinetics of Platelike Abnormal Grains in Liquid-Phase-Sintered Alumina. *Journal of the American Ceramic Society, 73*(7), 2077-2085.

Ikegami, T., Iyi, N., & Sakaguchi, I. (2010). Influence of magnesia on sintering stress of alumina. *Ceramics International, 36*(3), 1143-1146. Johnson, W., & Coble, R. (1978). A Test of the Second-Phase and Impurity-Segregation Models for MgO-Enhanced Densification of Sintered Alumina. *Journal of the American Ceramic Society, 61*(3-4), 110-114.

Jorgensen, P. (1965). Modification of sintering kinetics by solute segregation in Al2O3. *Journal of the American Ceramic Society, 48*(4), 207-210.

Jorgensen, P., & Westbrook, J. (1964). Role of Solute Segregation at Grain Boundaries During Final–Stage Sintering of Alumina. *Journal of the American Ceramic Society, 47*(7), 332-338.

Kebbede, A., Messing, G. L., & Carim, A. H. (1997). Grain Boundaries in Titania-Doped α-Alumina with Anisotropic Microstructure. *Journal of the American Ceramic Society, 80*(11), 2814-2820.

Keski, J., & Cutler, I. (1968). Initial Sintering of MnXO-Al2O3. *Journal of the American Ceramic Society, 51*(8), 440-444.

Keski, J. R., & Cutler, I. B. (1965). Effect of manganese oxide on sintering of alumina. *Journal of the American Ceramic Society, 48*(12), 653-654.

Kim, B. K., Hong, S. H., Lee, S. H., Kim, D. Y., & Hwang, N. M. (2003). Alternative explanation for the role of magnesia in the sintering of alumina containing small amounts of a liquid phase. *Journal of the American Ceramic Society, 86*(4), 634-639.

Kim, D.-S., Lee, J.-H., Sung, R. J., Kim, S. W., Kim, H. S., & Park, J. S. (2007). Improvement of translucency in Al2O3 ceramics by two-step sintering technique. *Journal of the European Ceramic Society, 27*(13-15), 3629-3632.

Kirchheim, R. (2002). <Grain coarsening inhibited by solute segregation.pdf>. *Acta Materialia, 50*, 413 - 419.

Krell, A. (1998). A new look at the influences of load, grain size and grain boundaries on the room temperature hardness of ceramics. *International Journal of Refractory Metals and Hard Materials, 16*(4-6), 331-335.

Krell, A., & Blank, P. (1996). The Influence of shaping method on the grain size dependence of strength in dense submicrometre alumina. *Journal of the European Ceramic Society, 16*(11), 1189-1200.

Kwa, S., Ramesh, S., Bang, L., Wong, Y., Chew, W. K., Tan, C., . . . Teng, W. (2015). Effect of sintering holding time on the properties and low-temperature degradation behaviour of manganese oxide-doped Y-TZP ceramic. *Journal of Ceramic Processing Research, 16*(2), 193-198.

Lahiri, S., Sinhamahapatra, S., Tripathi, H. S., & Dana, K. (2016). Rationalizing the role of magnesia and titania on sintering of α-alumina. *Ceramics International, 42*(14), 15405-15413.

Lartigue-Korinek, S., Carry, C., & Priester, L. (2002). Multiscale aspects of the influence of yttrium on microstructure, sintering and creep of alumina. *Journal of the European Ceramic Society, 22*(9-10), 1525-1541.

Lartigue-Korinek, S., Legros, C., Carry, C., & Herbst, F. (2006). Titanium effect on phase transformation and sintering behavior of transition alumina. *Journal of the European Ceramic Society, 26*(12), 2219-2230. doi:10.1016/j.jeurceramsoc.2005.04.006

Le Gall, M., Huntz, A., Lesage, B., Monty, C., & Bernardini, J. (1995). Self-diffusion in α-Al 2 O 3 and growth rate of alumina scales formed by oxidation: effect of Y 2 O 3 doping. *Journal of Materials Science, 30*(1), 201-211.

Li, H., Souza, F. L., & Castro, R. H. R. (2017). Kinetic and thermodynamic effects of manganese as a densification aid in yttria-stabilized zirconia. *Journal of the European Ceramic Society*.

Li, H., Xi, X., Ma, J., Hua, K., & Shui, A. (2017). Low-temperature sintering of coarse alumina powder compact with sufficient mechanical strength. *Ceramics International, 43*(6), 5108-5114.

Liu, Y., Min, F.-f., Zhu, J.-b., & Zhang, M.-x. (2012). Effect of nanometer Al2O3 powder on microstructure and properties of alumina ceramics by microwave sintering. *Materials Science and Engineering: A, 546*, 328-331.

Lóh, N. J., Simão, L., Faller, C. A., De Noni, A., & Montedo, O. R. K. (2016). A review of two-step sintering for ceramics. *Ceramics International, 42*(11), 12556-12572.

Maca, K., Pouchlý, V., Bodišová, K., Švančárek, P., & Galusek, D. (2014). Densification of fine-grained alumina ceramics doped by magnesia, yttria and zirconia evaluated by two different sintering models. *Journal of the European Ceramic Society, 34*(16), 4363-4372.

Maca, K., Pouchly, V., & Zalud, P. (2010). Two-step sintering of oxide ceramics with various crystal structures. *Journal of the European Ceramic Society, 30*(2), 583-589.

Macaigne, R., Marinel, S., Goeuriot, D., Meunier, C., Saunier, S., & Riquet, G. (2016). Microwave sintering of pure and TiO 2 doped MgAl 2 O 4 ceramic using calibrated, contactless in-situ dilatometry. *Ceramics International, 42*(15), 16997-17003. Manshor, H., Abdullah, E. C., Azhar, A. Z. A., Sing, Y. W., & Ahmad, Z. A. (2017). Microwave sintering of zirconia-toughened alumina (ZTA)-TiO 2 -Cr 2 O 3 ceramic composite: The effects on microstructure and properties. *Journal of Alloys and Compounds, 722*, 458-466.

Mazaheri, M., Zahedi, A. M., & Hejazi, M. M. (2008). Processing of nanocrystalline 8mol% yttria-stabilized zirconia by conventional, microwave-assisted and two-step sintering. *Materials Science and Engineering: A, 492*(1-2), 261-267.

Meenaloshini, S., Amiriyan, M., Sankar, U., Tolouei, R., & Ramesh, S. (2011). *The Influence of Manganese Oxide on the Sintering Behavior of Yttria Tetragonal Zirconia.* Paper presented at the AIP Conference Proceedings.

Mendelson, M. I. (1969). Average grain size in polycrystalline ceramics. *Journal of the American Ceramic Society, 52*(8), 443-446.

Menezes, R., & Kiminami, R. (2008). Microwave sintering of alumina–zirconia nanocomposites. *Journal of materials processing technology, 203*(1-3), 513-517.

Miaofang, C., Hui, G., Xin, W., & Peiling, W. (2003). Evidence of Bilevel Solubility in the Bimodal Microstructure of TiO2-Doped Alumina. *Journal of the American Ceramic Society, 86*(11), 1953-1955.

Mishra, R., Mukherjee, A., Yamazaki, K., & Shoda, K. (1996). Effect of TiO 2 doping on rapid densification of alumina by plasma activated sintering. *Journal of Materials Research, 11*(5), 1144-1148.

Mollá, J., Moreno, R., & Ibarra, A. (1996). Effect of Mg doping on dielectric properties of alumina. *Journal of Applied Physics, 80*(2), 1028-1032.

Monaco, C., Prete, F., Leonelli, C., Esposito, L., & Tucci, A. (2015). Microstructural study of microwave sintered zirconia for dental applications. *Ceramics International, 41*(1), 1255-1261.

Morteza Oghbaei, & Omid Mirzaee. (2010). <Microwave versus conventional sintering A review of fundamentals,.pdf>. *Journal of Alloys and Compounds*. Muche, D. N. F., Drazin, J. W., Mardinly, J., Dey, S., & Castro, R. H. R. (2017). Colossal grain boundary strengthening in ultrafine nanocrystalline oxides. *Materials Letters, 186*, 298-300.

Munir, Z. A., Anselmi-Tamburini, U., & Ohyanagi, M. (2006). The effect of electric field and pressure on the synthesis and consolidation of materials: A review of the spark plasma sintering method. *Journal of Materials Science, 41*(3), 763-777.

Nafsin, N., & Castro, R. H. R. (2016). Direct measurements of quasi-zero grain boundary energies in ceramics. *Journal of Materials Research, 32*(01), 166-173.

Nakagawa, T., Sakaguchi, I., Shibata, N., Matsunaga, K., Mizoguchi, T., Yamamoto, T., . . . Ikuhara, Y. (2007). Yttrium doping effect on oxygen grain boundary diffusion in α-Al2O3. *Acta Materialia, 55*(19), 6627-6633.

Nanni, P., Stoddart, C., & Hondros, E. (1976). Grain boundary segregation and sintering in alumina. *Materials Chemistry, 1*(4), 297-320.

Ng, C., Ramesh, S., Tan, C., Ching, C., Lwin, N., & Muchtar, A. (2016). Effect of manganese oxide on the densification and properties of ceria-doped scandia stabilized zirconia. *Journal of Ceramic Processing Research, 17*(5), 443-447.

Nishiyama, N., Taniguchi, T., Ohfuji, H., Yoshida, K., Wakai, F., Kim, B.-N., . . . Funakoshi, K.-i. (2013). Transparent nanocrystalline bulk alumina obtained at 7.7GPa and 800°C. *Scripta Materialia, 69*(5), 362-365.

Oghbaei, M., & Mirzaee, O. (2010). Microwave versus conventional sintering: a review of fundamentals, advantages and applications. *Journal of Alloys and Compounds, 494*(1), 175-189.

Patrick, W. S., & Cutler, I. B. (1965). Grain growth in sintered alumina. *Journal of the American Ceramic Society, 48*(10), 541-542.

Peng, Z., Hwang, J.-Y., & Andriese, M. (2013). Design of double-layer ceramic absorbers for microwave heating. *Ceramics International, 39*(6), 6721-6725.

Pereira, G. J., Bolis, K., Muche, D. N. F., Gouvêa, D., & Castro, R. H. R. (2017). Direct measurement of interface energies of magnesium aluminate spinel and a brief sintering analysis. *Journal of the European Ceramic Society, 37*(13), 4051-4058.

Pereira, G. J., Castro, R. H. R., de Florio, D. Z., Muccillo, E. N. S., & Gouvêa, D. (2005). Densification and electrical conductivity of fast fired manganese-doped ceria ceramics. *Materials Letters, 59*(10), 1195-1199.

Pillai, S. K. C., Baron, B., Pomeroy, M. J., & Hampshire, S. (2004). Effect of oxide dopants on densification, microstructure and mechanical properties of alumina-silicon carbide nanocomposite ceramics prepared by pressureless sintering. *Journal of the European Ceramic Society, 24*(12), 3317-3326. Radonjić, L., & Srdić, V. (1997). Effect of magnesia on the densification behavior and grain growth of nucleated gel alumina. *Materials chemistry and physics, 47*(1), 78-84.

Rahaman, M., & Zhou, Y. (1995). Effect of solid solution additives on the sintering of ultra-fine CeO2 powders. *Journal of the European Ceramic Society, 15*(10), 939-950.

Ramesh, S., Amiriyan, M., Meenaloshini, S., Tolouei, R., Hamdi, M., Pruboloksono, J., & Teng, W. D. (2011). Densification behaviour and properties of manganese oxide doped Y-TZP ceramics. *Ceramics International, 37*(8), 3583-3590.

Ramesh, S., Chew, W. K., Tan, C., Purbolaksono, J., Noor, A., Hassan, M., . . . Teng, W. (2013). Influence of manganese on the sintering properties of tetragonal zirconia. *Ceramics–Silikáty, 57*(1), 28-32.

Ramesh, S., Meenaloshini, S., Tan, C. Y., Chew, W. J. K., & Teng, W. D. (2008). Effect of manganese oxide on the sintered properties and low temperature degradation of Y-TZP ceramics. *Ceramics International, 34*(7), 1603-1608.

Ramesh, S., Tan, C. Y., Peralta, C. L., & Teng, W. D. (2016). The effect of manganese oxide on the sinterability of hydroxyapatite. *Science and Technology of Advanced Materials, 8*(4), 257-263.

Ramesh, S., Zulkifli, N., Tan, C. Y., Wong, Y. H., Tarlochan, F., Ramesh, S., . . . Sarhan, A. A. D. (2018). Comparison between microwave and conventional sintering on the properties and microstructural evolution of tetragonal zirconia. *Ceramics International.*

Roy, S. K., & Coble, R. L. (1968). Solubilities of magnesia, titania, and magnesium titanate in aluminum oxide. *Journal of the American Ceramic Society, 51*(1), 1-6.

Rybakov, K. I., Eremeev, A. G., Egorov, S. V., Bykov, Y. V., Pajkic, Z., & Willert-Porada, M. (2008). Effect of microwave heating on phase transformations in nanostructured alumina. *Journal of Physics D: Applied Physics, 41*(10), 102008.

Rybakov, K. I., & Semenov, V. E. (1995). Mass transport in ionic crystals induced by the ponderomotive action of a high-frequency electric field. *Physical Review B, 52*(5), 3030-3033. Sathiyakumar, M., & Gnanam, F. D. (2002). Influence of MnO and TiO2 additives on density, microstructure and mechanical properties of Al2O3. *Ceramics International, 28*, 195-200.

Sato, E., & Carry, C. (1993). Sintering and yttrium grain boundary segregation in sub-micron grain size alumina. *Le Journal de Physique IV, 3*(C7), C7-1335-C1337-1340.

Sato, E., & Carry, C. (1996). Yttria Doping and Sintering of Submicrometer-Grained α-Alumina. *Journal of the American Ceramic Society, 79*(8), 2156-2160.

Scott, C., Kaliszewski, M., Greskovich, C., & Levinson, L. (2002). Conversion of Polycrystalline Al2O3 into Single-Crystal Sapphire by Abnormal Grain Growth. *Journal of the American Ceramic Society, 85*(5), 1275-1280.

Seong-Hyeon, H., & Doh-Yeon, K. (2001). Effect of Liquid Content on the Abnormal Grain Growth of Alumina. *Journal of the American Ceramic Society, 84*(7), 1597-1600.

Song, K., Wu, S., & Chen, X. (2007). Effects of Y2O3 addition on microwave dielectric characteristics of Al2O3 ceramics. *Materials Letters, 61*(16), 3357-3360.

Song, K. X., Wu, S. Y., & Chen, X. M. (2007). Effects of Y2O3 addition on microwave dielectric characteristics of Al2O3 ceramics. *Materials Letters, 61*(16), 3357-3360.

Sopyan, I., Ramesh, S., Nawawi, N. A., Tampieri, A., & Sprio, S. (2011). Effects of manganese doping on properties of sol–gel derived biphasic calcium phosphate ceramics. *Ceramics International, 37*(8), 3703-3715.

Thuault, A., Savary, E., Hornez, J. C., Moreau, G., Descamps, M., Marinel, S., & Leriche, A. (2014). Improvement of the hydroxyapatite mechanical properties by direct microwave sintering in single mode cavity. *Journal of the European Ceramic Society, 34*(7), 1865-1871.

Tianshu, Z., Hing, P., Huang, H., & Kilner, J. (2001). Sintering and densification behavior of Mn-doped CeO2. *Materials Science and Engineering: B, 83*(1-3), 235-241.

Venkatesh, M., & Raghavan, G. (2004). An overview of microwave processing and dielectric properties of agri-food materials. *Biosystems Engineering, 88*(1), 1-18.

Vongpradubchai, S., & Rattanadecho, P. (2009). The microwave processing of wood using a continuous microwave belt drier. *Chemical Engineering and Processing: Process Intensification, 48*(5), 997-1003.

Wang, J., Binner, J., Pang, Y., & Vaidhyanathan, B. (2008). Microwave-enhanced densification of sol–gel alumina films. *Thin Solid Films, 516*(18), 5996-6001.

Wang, J., Binner, J., Vaidhyanathan, B., Joomun, N., Kilner, J., Dimitrakis, G., & Cross, T. (2006). Evidence for the microwave effect during hybrid sintering. *Journal of the American Ceramic Society, 89*(6), 1977-1984.

Wei Chang, I., & Wang, X. H. (2000). Sintering dense nanocrystalline ceramics without final-stage grain growth *Nature, 404*, 168-171.

Weissmüller, J. (1993). Alloy effects in nanostructures. *Nanostructured Materials, 3*(1-6), 261-272.

Wollmershauser, J. A., Feigelson, B. N., Gorzkowski, E. P., Ellis, C. T., Goswami, R., Qadri, S. B., . . . Everett, R. K. (2014). An extended hardness limit in bulk nanoceramics. *Acta Materialia, 69*, 9-16.

Wroe, R., & Rowley, A. (1996). Evidence for a non-thermal microwave effect in the sintering of partially stabilized zirconia. *Journal of Materials Science, 31*(8), 2019-2026.

Wu, L., Aguiar, J. A., Dholabhai, P. P., Holesinger, T., Aoki, T., Uberuaga, B. P., & Castro, R. H. R. (2015). Interface Energies of Nanocrystalline Doped Ceria: Effects of Manganese Segregation. *The Journal of Physical Chemistry C, 119*(49), 27855-27864.

Wu, L., Dey, S., Gong, M., Liu, F., & Castro, R. H. R. (2014). Surface Segregation on Manganese Doped Ceria Nanoparticles and Relationship with Nanostability. *The Journal of Physical Chemistry C, 118*(51), 30187-30196.

Wu, L., Dholabhai, P. P., Uberuaga, B. P., & Castro, R. H. (2017). Temperature Dependence Discontinuity in the Stability of Manganese-Doped Ceria Nanocrystals. *Crystal Growth & Design, 17*(2), 446-453.

Xie, Z., Yang, J., & Huang, Y. (1998). Densification and grain growth of alumina by microwave processing. *Materials Letters, 37*, 215-220.

Xu, W., Yin, Z., Yuan, J., Wang, Z., & Fang, Y. (2017). Effects of sintering additives on mechanical properties and microstructure of Si3N4 ceramics by microwave sintering. *Materials Science and Engineering: A, 684*, 127-134.

Yin, Z., Yuan, J., Cheng, Y., Zhang, Y., Wang, Z., & Hu, X. (2016). Microstructure evolution and densification kinetics of Al 2 O 3 /Ti(C,N) ceramic tool material by microwave sintering. *International Journal of Refractory Metals and Hard Materials, 61*, 225-229.

Young-Min, K., Seong-Hyeon, H., & Doh-Yeon, K. (2000). Anisotropic Abnormal Grain Growth in TiO2/SiO2-Doped Alumina. *Journal of the American Ceramic Society, 83*(11), 2809-2812.

Zhang, T., Chan, S., Wang, W., Hbaieb, K., Kong, L., & Ma, J. (2009). Effect of Mn addition on the densification, grain growth and ionic conductivity of pure and SiO2-containing 8YSZ electrolytes. *Solid State Ionics, 180*(1), 82-89.

Zhang, T., Hing, P., Huang, H., & Kilner, J. (2002). Sintering study on commercial CeO2 powder with small amount of MnO2 doping. *Materials Letters, 57*(2), 507-512.

Zhang, T., Kong, L., Zeng, Z., Huang, H., Hing, P., Xia, Z., & Kilner, J. (2003). Sintering behavior and ionic conductivity of Ce0.8Gd0.2O1.9 with a small amount of MnO2 doping. *Journal of Solid State Electrochemistry, 7*(6), 348-354. Zhang, T. S., Du, Z. H., Li, S., Kong, L. B., Song, X. C., Lu, J., & Ma, J. (2009). Transitional metal-doped 8 mol% yttria-stabilized zirconia electrolytes. *Solid State Ionics, 180*(23-25), 1311-1317.

Zhang, T. S., Kong, L. B., Du, Z. H., Ma, J., & Li, S. (2010). Tailoring the microstructure of mechanoactivated Al2O3 and SiO2 mixtures with TiO2 addition. *Journal of Alloys and Compounds, 506*(2), 777-783.

Zhao, C., vleugels, J., Groffils, C., Luypaert, P. J., & Van Der Biest, O. (2000). hybrid sintering with a tubular susceptor in a cylindrical single mode microwave furnace. *Acta Materialia, 48*, 3795-3801.

Zhao, J., & Harmer, M. P. (1987). Sintering of Ultra-High-Purity Alumina Doped Simultaneously with MgO and FeO. *Journal of the American Ceramic Society, 70*(12), 860-866.

Zhou, H., Li, J., Yi, D., & Xiao, L. (2011). Effect of manganese oxide on the sintered properties of 8YSZ. *Physics Procedia, 22*, 14-19.

Zong, L., Zhou, S., Sgriccia, N., Hawley, M., & Kempel, L. (2003). A Review of Microwave-Assist Polymer Chemistry (MAPC). *Journal of Microwave Power and Electromagnetic Energy, 38*(1), 49-74.

Zuo, F., Badev, A., Saunier, S., Goeuriot, D., Heuguet, R., & Marinel, S. (2014). Microwave versus conventional sintering: Estimate of the apparent activation energy for densification of α-alumina and zinc oxide. *Journal of the European Ceramic Society, 34*(12), 3103-3110.

Zuo, F., Carry, C., Saunier, S., Marinel, S., Goeuriot, D., & Bordia, R. (2013). Comparison of the Microwave and Conventional Sintering of Alumina: Effect of MgO Doping and Particle Size. *Journal of the American Ceramic Society, 96*(6), 1732-1737. doi:10.1111/jace.12320

Zuo, F., Saunier, S., Marinel, S., Chanin-Lambert, P., Peillon, N., & Goeuriot, D. (2015). Investigation of the mechanism(s) controlling microwave sintering of α-alumina: Influence of the powder parameters on the grain growth, thermodynamics and densification kinetics. *Journal of the European Ceramic Society, 35*(3), 959-970.

Żymełka, D., Saunier, S., Goeuriot, D., & Molimard, J. (2013). Densification and thermal gradient evolution of alumina during microwave sintering at 2.45GHz. *Ceramics International, 39*(3), 3269-3277.

LIST OF PUBLICATIONS AND PAPERS PRESENTED

1. Dhuban, S. B., Ramesh, S., Tan, C. Y., Wong, Y. H., Johnson Alengaram, U., Ramesh, S., . . . Sutharsini, U. (2019). Sintering behaviour and properties of manganese-doped alumina. Ceramics International, 45(6), 7049-7054.